Characterization of the Critical Biochemical and Physiological Role of 1-Acylglycerol-3-Phosphate-O-Acyltransferase 4 (AGPAT4) in White Adipose Tissue

by
Emily Mardian

A thesis
presented to the University of Waterloo
in fulfillment of the
thesis requirement for the degree of
Master of Science
in
Kinesiology

Waterloo, Ontario, Canada, 2016

Author's Declaration

This thesis consists of material all of which I authored or co-authored: see Statement of Contributions included in the thesis. This is a true copy of the thesis, including any required final revisions, as accepted by my examiners.

I understand that my thesis may be made electronically available to the public.

Emily Mardian

Statement of Contributions

Parts of this thesis contains materials from a paper submitted to the Journal of Lipid Research. I would like to acknowledge the co-authors who contributed to the research described in this dissertation:

- Ryan M. Bradley
- Juan J. Aristizabal Henao
- Dr. Eric Bombardier
- Dr. A. Russell Tupling
- Dr. Ken D. Stark
- Dr. Robin E. Duncan

Abstract

White adipose tissue (WAT) is an endocrine and lipid storage organ that is imperative to mammals for the maintenance of energy homeostasis. WAT depot size and triacylglycerol (TAG) content is determined by the regulation of lipid metabolism in adipocytes, as well as by the number of adipocytes. The two main processes in TAG metabolism are hydrolysis (or lipolysis), and synthesis, which encompasses both *de novo* fatty acid synthesis, and complex lipid synthesis via the Kennedy pathway. The number of adipocytes is regulated primarily by adipogenesis, the differentiation of preadipocytes into fully mature adipocytes. Dysregulation of adipocyte lipid metabolism or adipogenesis can lead to pathological conditions such as obesity, diabetes, and cardiovascular disease. Thus, the maintenance of a healthy physiological state is critically dependent on normal adipose tissue development and function. The 1-acylglycerol-3-phosphate-O-acyltransferases (AGPATs) catalyze the second step in the Kennedy pathway, acylating lysophosphatidic acid (LPA) with a fatty acyl-CoA at the *sn-2* position, forming phosphatidic acid (PA). LPA and PA are bioactive signalling molecules that may affect the differentiation of adipocytes, while PA is also a building block for the synthesis of TAG and phospholipids that are components of expanding adipocytes. Changes in the activity of cellular AGPATs may therefore affect adipose tissue biology through multiple mechanisms. Little is known however, about the role of most of the AGPAT homologues in WAT. In this study, we aimed to better understand the *in vivo* function of AGPAT homologue 4 (AGPAT4) in WAT by using a gene ablation model of *Agpat4* to assess the role of this enzyme in three important white adipose tissue regulatory processes: lipogenesis, adipogenesis, and lipolysis. It was hypothesized that lack of AGPAT4 would reduce TAG synthesis, resulting in decreased whole body weights due to reductions in individual adipose tissue depot masses. Since TAG synthesis is required for adipocyte differentiation, it was further hypothesized that loss of AGPAT4 would impair differentiation. We predicted a compensatory reduction in adipocyte lipolysis would also be observed. Contrary to these predictions, it was found that AGPAT4 ablation resulted in a 40% increase in the mass of epididymal WAT, without causing a significant change in whole body weights, food intake, activity, oxygen consumption, or substrate oxidation. This was accompanied by a 26% increase in TAG content in epididymal WAT and an increase in the average adipocyte size within this depot, with no observed changes in the gene expression of adipogenic markers. The expression of genes encoding LIPIN1 and DGAT1 showed significant upregulation in epididymal WAT however, there were no changes in gene expression or protein content of other markers of lipogenesis. *Agpat4*$^{-/-}$ epididymal WAT showed a decrease in ATGL, P-HSL S563, and P-HSLS660 content, decreased total triolein lipase activity, and dibutyryl-cAMP stimulated glycerol release,

indicating a decrease in lipolytic activity. In contrast, no differences in any measures of lipogenesis, lipolysis, or adipogenesis were observed for perirenal WAT with the exception of a compensatory upregulation of the other AGPAT isoforms. Notably, this compensation was not observed in epididymal WAT, which paradoxically exhibited an increase in PA content. Our findings suggest that induction of the other AGPAT isoforms may be responsible for maintaining normal adipocyte differentiation and function in perirenal WAT, but that this compensation does not occur in epididymal WAT, which consequently becomes dysregulated.

Acknowledgements

First and Foremost, I would like to extend my sincerest appreciation to my supervisor, Dr. Robin Duncan, for her continuous guidance and support throughout my undergraduate and graduate careers. I am so grateful for the vast opportunities and the unrelenting encouragement she has provided over the past three years as without it, I know I would not be in the position I am in today. Thank you for believing in me since day one. Most importantly, I am incredibly thankful to have been able to work with such a fantastic, intelligent, and passionate professor.

I would also like to thank my committee members, Dr. Ken Stark and Dr. A Russell Tupling, for their insights and recommendations throughout my project, as well as the past and present members of my lab. To Ryan Bradley, Kristin Marks, Katy Moes, and Phil Marvyn, I couldn't think of a better group of people to sit across from, learn, and laugh with each and every day. I'd like to further extend my thanks to Ryan Bradley, for being the greatest mentor and teacher I could have asked for but more importantly, for being a great friend, big brother, and support system. Thank you Juan J. Aristizabal Henao for being our honourary lab member and for all his willingness to help with the gas chromatography experiments. As well as to Dr. Eric Bombardier for all his help with the CLAMS experiments. I'd also like to thank every other member of physiology, I'm so thankful to have had the opportunity to spend every day with the most kind and intelligent group of people.

I'd also like to thank my friends and family for their love, encouragement, and unwavering support as I've chased my dreams. In particular, to my mother and George, my siblings Ben, Jacob, and Kaitlyn, and the most wonderful new addition to our family, my niece Madison. Last, but certainly not least, thank you a million times over to my best friends Hilary Simon and Darin Bloemberg for being my rocks and rays of sunshine every single day.

Table of Contents

List of Tables

List of Figures

List of Abbreviations

ADIPOQ: Adiponectin, C1Q And Collagen Domain Containing
AGPAT: 1-acylglycerol-3-phosphate-O-acyltransferase
ALCAT1: acyl-CoA:lysocardiolipin acyltransferase-1
AMPK: 5' adenosine monophospohate-activated protein kinase
aP2/FABP4: adipocyte protein 2/fatty acid binding protein 4
ATGL: adipose-triglyceride lipase
BAT: brown adipose tissue
BCA: bicinchoninic acid
BSA: bovine serum albumin
cAMP: cyclic adenosine monophosphate
CDP-DAG: cytidine diphosphate-diacylglycerol
CDS: CDP-DAG synthase
C/EBP: CCAAT/enhancer-binding proteins
CGL: congenital generalized lipodystrophy
CL: cardiolipin
CLAMS: Comprehensive Laboratory Animal Monitoring System
CLS: cardiolipin synthase
CMP: cytidine monophosphate
CoA: coenzyme A
CPT: CDP-choline: 1,2-diacylglycerol cholinephosphotransferase
CTP: cytidine triphosphate
DAG: diacylglycerol
DGAT: diacyglycerol acyltransferase
DHA: docosahexaenoic acid
DLCL: dilysocardiolipin
EPT: CDP-ethanolamine: 1,2-diacylglycerol ethanolaminephosphotransferase
FA: fatty acid
FAS: fatty acid synthase
G3P: glycerol-3-phosphate
GC: gas chromatography
GPAT: glycerophosphate acyltransferase
HRP: horseradish peroxidase
HSL: hormone-sensitive lipase
LPA: lysophosphatidic acid
LPAAT: lysophosphatidic acid acyltransferase
LPC: lysophosphatidylcholine
LPCAT: acyl-CoA:lysophosphatidylcholine acyltransferase
LPE: lysophosphaditylethanolamine
LPEAT: acyl-CoA:lysophoshatidylethanolamine
LPI: lysophosphatidylinositol
LPS: lysophosphatidylserine
MAG: monoacylglyceride
MAM: mitochondria-associated membrane
MBOAT: membrane-bound O-acyltransferase
MGL: monoglycerol lipase
MLCAT: acyl-CoA-dependent MLCL acyltransferase
MLCL: monolysocardiolipin

MUFA: monounsaturated fatty acids
NEFA: non-esterified fatty acid
PA: phosphatidic acid
PAF: platelet-activating factor
PAFAT: platelet-activating factor acetyltransferase
PAP: phosphatidic acid phosphohydrolase
PC: phosphatidylcholine
PE: phosphatidylethanolamine
PG: phosphatidylglycerophosphate
PGP: phosphatidylglycerol phosphate
PGPS: phosphatidylglycerophosphate synthase
PI: phosphatidylinositol
PIS: phosphatidylinositol synthase
PKA: protein kinase A
PPAR: peroxisome proliferator-activated receptor
PREF-1: preadipocyte factor 1
PS: phosphatidylserine
PSS: phosphatidylserine synthase
PTPMT: protein tyrosine phosphatase, mitochondrial
PUFA: polyunsaturated fatty acid
RER: respiratory exchange ratio
SREBP: sterol response element-binding protein
STAT: single transducers and activators of transcription
TAE: tris-acetate-EDTA
TAG: triacylglycerol
TLC: thin layer chromatography
TZD: thiazolidinedione
VLDL: very low density lipoprotein
WAT: white adipose tissue

Chapter 1: Introduction

White adipose tissue (WAT) is an endocrine organ that is imperative to mammals for the maintenance of energy homeostasis. It is a form of loose connective tissue composed of specialized cells, known as adipocytes, as well as nerve tissue, stromovascular cells, and immune cells (1). Together, these components form an integrative unit that acts as an energy reserve, as thermal insulation, and as an endocrine organ involved in adipokine signaling throughout the body (2, 3). WAT is distributed throughout the body in several regional depots that have known differences in size, organization, and biological function. The main depots include visceral WAT, the adipose tissue surrounding inner organs in the thoracic and abdominal cavities, as well as subcutaneous WAT, the adipose tissue directly beneath the skin, which have been shown to have different developmental origins (2, 4).

During a positive energy state, or energy excess, WAT stores energy in the form of triacylglycerol (TAG), which is composed of three fatty acyl chains esterified to a glycerol backbone. During a negative energy state, or energy deprivation, WAT hydrolyzes TAG, in a process termed lipolysis, to liberate glycerol and free fatty acids that can be used by other organs as energy substrates (5). WAT size and TAG content is determined by the regulation of lipid metabolism in adipocytes, including lipid synthesis and lipolysis, as well as adipogenesis, the process in which adipocytes differentiate into fully mature adipocytes from precursor preadipocytes. Dysregulation of any one of these processes can lead to detrimental disorders (1). In particular, obesity, which is caused by excess WAT, and is rising in prevalence, is associated with metabolic disorders, such as type II diabetes and dyslipidemia, hypertension, atherosclerosis, and cardiovascular disease (6).

An increase in WAT, or fat mass, requires an increase in adipocyte size (hypertrophy) or an increase in adipocyte number (hyperplasia) (7). At least in the early stages, obesity primarily results from adipocyte *hypertrophy* rather than *hyperplasia*, and is caused when TAG synthesis exceeds TAG breakdown (7). Unlike most other cell types in the body, adipocytes are well suited to the storage of TAG and the expansion of adipocyte TAG stores is not immediately detrimental to health, *per se*. Rather, pathological conditions primarily ensue when the hypertrophic expansion of adipocytes results in hypoxia, fibrosis, and inflammation within the tissue, which can then cause insulin resistance (8, 9). These conditions are observed more frequently in hypertrophic visceral WAT depots and less often in subcutaneous WAT depots (10). As a result, visceral WAT mass tends to correlate with the development of insulin resistance, whereas total adipose tissue depot size, and

the size of subcutaneous adipose tissue, does not (5, 10). This has been attributed to multiple factors such as differing degrees of inflammation, levels of adipokines, and response to insulin-sensitizing compounds such as thiazolidinediones (TZDs). The higher metabolic activity of visceral WAT has also been suggested as a factor linking this depot to the development of pathological conditions in obesity. Visceral WAT has been shown to have greater mitochondrial content, higher rates of oxidative phosphorylation, higher rates of lipolysis, as well as higher insulin-stimulated glucose uptake per weight of fat mass (10-13). Therefore, visceral WAT may contribute more to the levels of plasma free fatty acids than subcutaneous WAT, as well as enhanced free fatty acid delivery to the liver, resulting in increased very low density lipoprotein (VLDL) output and impaired hepatic insulin response (10). It has therefore been suggested that subcutaneous WAT may provide a greater and more metabolically beneficial storage capacity for TAG (10). Within both subcutaneous and visceral WAT however, are several distinct depots anatomically separated from one another. For example, visceral WAT is composed of six depots: gonadal/epididymal, perirenal, epicardial, retroperitoneal, omental, and mesenteric, and little is known about their individual biochemical properties (4).

Expansion of WAT through hyperplasia, resulting from increased adipogenesis, tends to occur with ascending obesity. It has been suggested that hyperplasia may follow hypertrophy in adipocytes once they have reached a maximum size, or critical volume (2). Hyperplasia therefore, may provide an adaptive and protective role to maintain insulin sensitivity (9). Indeed, increased adipocyte differentiation is a component of the insulin sensitizing action of some pharmaceutical agents, such as TZDs (14, 15). Conversely, lipodystrophy, which is characterized by a lack of WAT due to impaired TAG biosynthesis, accelerated TAG hydrolysis, or inadequate adipogenesis, is associated with insulin resistance, diabetes, and subsequent metabolic complications (16, 17). Thus, proper development, regulation, and maintenance of WAT cell number and TAG content is necessary for metabolic health, and understanding the factors underlying these processes may help provide treatment options for metabolic disease. It is therefore imperative to understand the biochemical pathways and enzymatic regulation of TAG. The acylglycerophosphate acyltransferase (AGPAT) group of enzymes function in the second step of the Kennedy pathway for the *de novo* synthesis of glycerolipids and TAG. The AGPAT isoforms show differential tissue distribution, but the physiological significance of this distribution, and the role of each isoform in different tissues including WAT, is not well understood (18). AGPAT isoform 4 (AGPAT4) shows evidence of expression in WAT, but its biochemical properties and physiological importance in this tissue have yet to be investigated.

Chapter 2: Biochemical Foundations

Lipolysis

Lipolysis is the sequential hydrolysis of TAG via the action of lipases, resulting in the release of a fatty acid at each step. Adipose-triglyceride lipase (ATGL) is the major enzyme involved in the hydrolysis of TAG (5). It is located both in the cytoplasm and on the lipid droplet where it preferentially cleaves a fatty acyl chain from the *sn-2* position of TAG, forming diacylglycerol (DAG) (19). Hormone-sensitive lipase (HSL) subsequently cleaves a fatty acyl chain from the *sn-1* or *sn-3* position of DAG (19). Similar to ATGL, HSL is also a cytoplasmic lipase, but it translocates to the lipid droplet when activated by the phosphorylation of protein kinase A (PKA) (20). Hydrolysis of DAG results in the formation of monoacylglycerol (MAG) that is hydrolyzed by monoglyceride lipase (MGL) in the cytosol to liberate glycerol and the final fatty acyl chain (5).

This process is regulated under hormonal control where, in times of energy excess, insulin acts to inhibit lipolysis, and in times of energy deprivation, catecholamines and glucocorticoids act to stimulate it (21). Catecholmines activate Gα-coupled receptors which stimulate adenylate cyclase, resulting in increased intracellular cyclic adenosine monophosphate (cAMP) concentrations. Increased cAMP levels activate cAMP-dependent PKA resulting in the phosphorylation of HSL at serine residues 563, 659, and 600, and increased hydrolytic activity at the lipid droplet (21). HSL may also be phosphorylated at serine site 565 by 5'adenosine monophosphate-activated protein kinase (AMPK), a cellular energy sensor (5, 21, 22). The action of HSL is also mediated by the lipid droplet-associated protein, perilipin A. When phosphorylated by the action of PKA, perilipin A has been shown to result in increased activity of HSL, perhaps through facilitation of HSL translocation to the lipid droplet, although findings have been variable (5, 23, 24). Glucocorticoids have been shown to induce ATGL expression. However, ATGL activity does not appear to be mediated by PKA or by translocation, since it is localized to the lipid droplet under both basal and hormonally stimulated conditions (21). AMPK has been shown to phosphorylate and activate ATGL, thereby stimulating lipolysis (22, 25).

Adipogenesis

Adipogenesis describes the development of an undifferentiated mesenchymal cell into a preadipocyte, which undergoes changes in morphology and gene expression to become a mature, lipid filled, insulin-responsive adipocyte (17). Adipocyte differentiation occurs during embryonic development, and although TAG storage in adipocytes largely results in increased adipocyte size, it

may also result in increased adipocyte differentiation (2). Adipogenesis is regulated by various classes of transcription factors which include sterol response element-binding proteins (SREBPs), the peroxisome proliferator-activated receptor (PPAR) family proteins, CCAAT/enhancer-binding proteins (C/EBPs), and signal transducers and activators of transcription (STATs) (17). Two of the transcription factors most commonly analyzed when assessing adipocyte differentiation are C/EBPα and PPARγ, since these nuclear factors are central to adipogenesis. Preadipocyte factor 1 (PREF-1) is an anti-adipogenic protein that directly regulates C/EBPβ and C/EBPδ (17). C/EBPβ and C/EBPδ target the promoters of genes for SREBP1, C/EBPα, as well as PPARγ, which subsequently form a heterodimer with the retinoid X receptor and bind to the DNA of various genes involved in adipogenesis. These include C/EBPα (which creates a positive feedback loop), aP2/FABP4 (adipocyte protein 2/fatty acid binding protein 4), ADIPOQ (Adiponectin, C1Q And Collagen Domain Containing), fatty acid synthase (FAS), perilipin, and AGPAT2 (17, 26).

The Kennedy pathway of complex glycerolipid synthesis

Glycerolipid synthesis occurs in the Kennedy pathway, which was first described by Eugene Kennedy in 1956 (27). The enzymes in this pathway regulate the production of TAG and the phospholipids phosphatidic acid (PA), phosphatidylcholine (PC), phosphaditylethanolamine (PE), phosphatidylglycerol (PG), phosphatidylinositol (PI), and cardiolipin (CL), and also influence the unique fatty acid composition of these lipid species (Fig. 1) (27, 28). The Kennedy pathway begins with the formation of glycerol-3-phosphate (G3P), an intermediate derived from the glycolysis pathway, since most extra-hepatic tissues lack significant glycerol kinase activity and therefore, cannot directly activate (or reactivate) glycerol. The first committal step of the Kennedy pathway is the acylation of G3P to produce 1-acylglycerol-3-phosphate, also known as lysophosphatidic acid (LPA). This is achieved by one of the four members of the glycerophosphate acyltransferase (GPAT) family that transfer a fatty acyl-coenzyme A (CoA) to the *sn-1* position of G3P. GPATs have the lowest specificity for enzymatic activity of all the enzymes involved in the Kennedy pathway (29). These enzymes catalyze both the initial and the rate limiting step in glycerolipid synthesis (29). Following the acylation of G3P, a fatty acid is transferred from an acyl-CoA to the *sn-2* position of the glycerol backbone of LPA to produce PA. This reaction is catalyzed by a member of the 1-acylglycerol-3-phosphate-O-acyltransferase (AGPAT) family, also known as a lysophosphatidic acid acyltransferase (LPAAT) (30). PA is an important branching point in the Kennedy pathway since it acts as the precursor to all membrane glycerophospholipids and TAG in mammals. PA can be shunted into one of two pathways. One pathway begins with the production of cytidine diphosphate-

diacylglycerol (CDP-DAG) ultimately leading to the production of PI, PG, or CL (27). The alternative pathway begins with the production of DAG and ultimately leads to the production of PC, PE, PS, or to the production of TAG (31).

The pathway leading to the production of PI, PG, and CL begins with the condensation of cytidine triphosphate (CTP) with PA, as catalyzed by CDP-DAG synthase (CDS), also known as phosphatidate cytidylyltransferase, to produce CDP-DAG. CDG-DAG can react with inositol to produce PI, as catalyzed by phosphatidylinositol synthase (PIS), which is also known as CDP-DAG inositol 3-phosphatidyltransferase (32). CDP-DAG can also react with G3P to form phosphatidylglycerol phosphate (PGP), as catalyzed by phosphatidylglycerophosphate synthase (PGPS), and the phosphate group of PGP is subsequently hydrolyzed by a phosphatase, known as protein tyrosine phosphatase, mitochondrial 1 (PTPMT1) to produce PG. CDP-DAG becomes committed to the cardiolipin synthesis pathway when it becomes PGP (33). Cardiolipin synthase (CLS) then catalyzes the condensation of PG to CDP-DAG, with the elimination of cytidine monophosphate (CMP), to produce immature cardiolipin (27).

The pathway leading to the production of PE, PC, PS, or TAG begins with dephosphorylation of PA to produce DAG, as catalyzed by phosphatidic acid phosphohydrolase (PAP) also known as LIPIN1 (34). DAG can be used to produce PE through the addition of CDP-phosphoethanolamine, as catalyzed by CDP-ethanolamine: 1,2-diacylglycerol ethanolaminephosphotransferase (EPT), and to produce PC through the addition of CDP-choline, as catalyzed by CDP-choline: 1,2-diacylglycerol cholinephosphotransferase (CPT) (27). PS can be produced from PC in which the choline group is exchanged for a serine, as catalyzed by PS synthase-1 (PSS1), or from PE in which the ethanolamine group is exchanged from a serine, as catalyzed by PSS2 (35). To produce TAG, diacylglycerol acyltransferase (DGAT) catalyzes the conversion of DAG to TAG through esterification primarily at the *sn-1* or *sn-3* positions (36).

GPATs and AGPATs incorporate fatty acids into PA, which is the precursor of all other glycerophospholipids and TAG. The acyl-CoA specificity of these initial Kennedy pathway enzymes therefore, determines the fatty acyl composition of newly synthesized phospholipids and TAG (37, 38). After formation however, phospholipids can be remodelled to achieve a different final fatty acyl composition through the action of the Land's cycle (28). For example, arachidonic acid and other ≥C20 polyunsaturated fatty acids are not commonly incorporated into phospholipids during *de novo*

synthesis, but rather during phospholipid fatty acid remodeling (38). This remodeling is mediated by enzymes of the membrane-bound O-acyltransferase (MBOAT) family and by some homologues of the AGPAT family of enzymes (AGPAT7, 8, 9, 11), which have turned out to have greater specificity for lysophospholipids other than LPA (38).

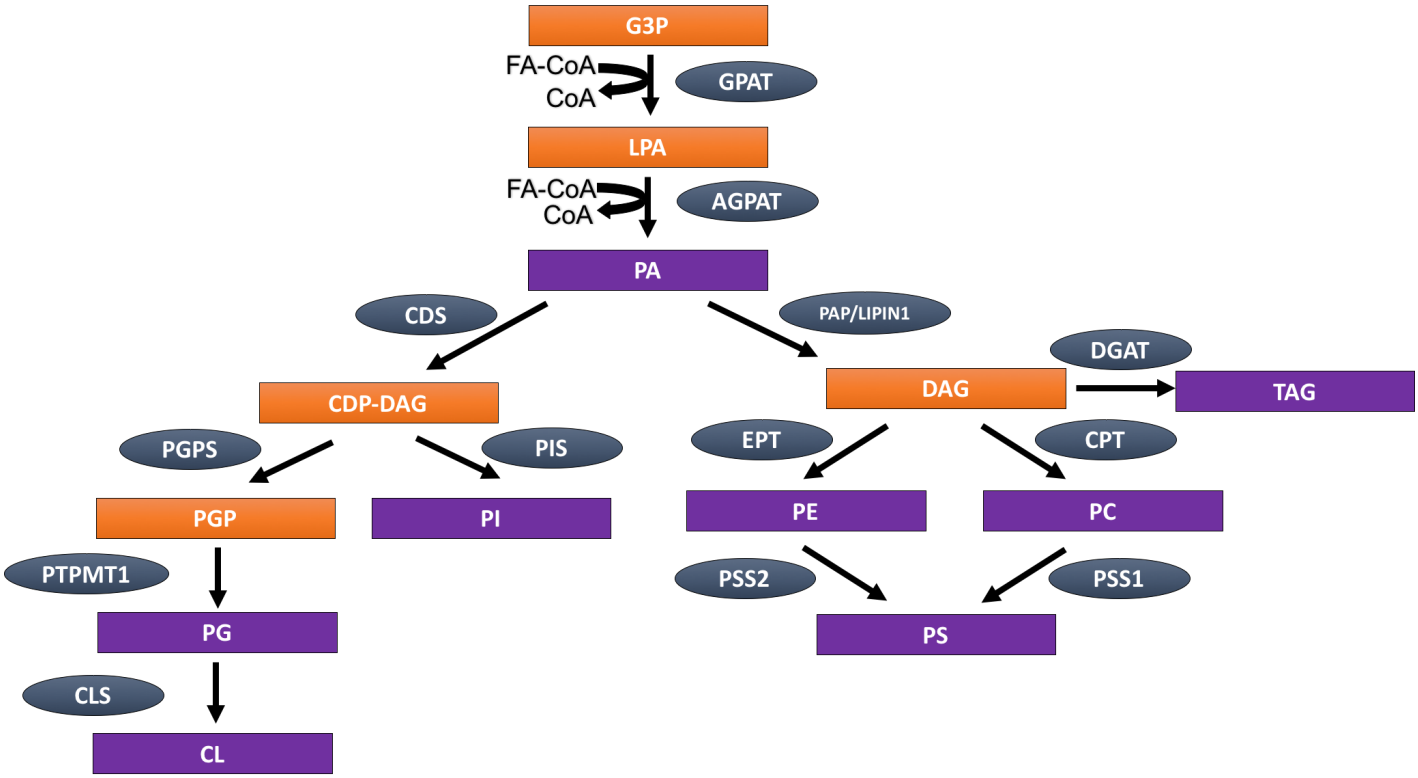

Figure 1. The Kennedy pathway for the de novo synthesis of triacylglycerol and phospholipids. Fatty acid = FA.

Glycerol-3-phosphate acyltransferases (GPATs)

Two mitochondrial GPAT isoenzymes have been identified which localize to the outer mitochondrial membrane. GPAT1 preferentially acylates G3P with saturated fatty acyl-CoAs rather than unsaturated fatty acyl-CoAs, while GPAT2 shows no preference for the fatty acyl-CoA species donor (39, 40). In contrast, the microsomal GPATs localize to the endoplasmic reticulum and have activity ten times higher than that of mitochondrial GPATs (39-43). GPAT3 was originally called AGPAT10, but has been renamed based on a preference for G3P over LPA as the acyl acceptor (44). GPAT3 has been found to use long-chain fatty acyl-CoAs as donors, but shows no preference between saturated or unsaturated species (41, 44). GPAT4 was originally called AGPAT6 (42). It also showed no preference between saturated and unsaturated fatty acyl species (42, 45).

1-acylgylcerol-3-phosphate-O-acyltransferases (AGPATs)

Eleven members of the AGPAT family of enzymes have thus far been identified in humans and mice, with each containing two highly conserved catalytic acyltransferase motifs, NHX_4D and a downstream proline residue, as well as two substrate (LPA) binding motifs, EGTR and FX_2R (18, 30, 44, 46-54). Most AGPATs have undergone subsequent renaming as additional information became available regarding substrate specificity, and now only five of these enzymes remain classified as true AGPATs that utilize LPA as their major fatty acyl acceptor. Others utilize G3P as their major acyl acceptor, thereby functioning as GPATs, or utilize other lysophospholipid species as acyl acceptors (42, 44, 45, 55-58).

In 1997, AGPAT1, also known as LPAATα, became the first murine AGPAT isoform to be cloned and characterized (30). It was found to be a true AGPAT that utilizes only LPA as its major fatty acyl acceptor while preferring acyl-CoA donors with chain lengths from 12 to 18 carbons with a preference for C18:1 and C18:2 (30, 46, 59). AGPAT1 also utilized C15:0, an odd chain fatty acid, for LPA acylation at a high rate (46). AGPAT1 is ubiquitously expressed in most tissues, with highest expression in the testis, pancreas, and adipose tissue, and it localizes to the endoplasmic reticulum (30, 46).

AGPAT2, also as known as LPAATβ, also utilizes LPA as its major fatty acyl acceptor and C18:1-CoA as its major fatty acyl donor, with activity for 16:0-CoA and 18:0-CoA as well. (46, 60). AGPAT2 is localized to the endoplasmic reticulum and shows expression in a tissue-specific manner, with highest expression in adipose tissue and lower levels of expression in the liver and pancreas (46).

AGPAT3 (LPAATγ) is localized to the endoplasmic reticulum, nuclear envelope, and Golgi apparatus, and shows highest expression in the testes (47, 61, 62). It prefers oleoyl-CoA (18:1n-9-CoA) and arachidonoyl-CoA (20:4n-6-CoA) as fatty acyl donors in the production of PA from LPA, but also shows acyltransferase activity towards lysophosphatidylcholine (LPC), lysophosphatidylserine (LPS), and lysophosphatidylinositol (LPI) in the presence of arachidonoyl-CoA as the fatty acyl donor (47, 62).

AGPAT4, also known as LPAATδ, shows acyltransferase activity with LPA, but not with any other major lysophospholipids (48). AGPAT4 preferentially esterifies saturated fatty acyl-CoA species to LPA, particularly C12:0 and C20:0 (48, 63). It is localized to the outer mitochondrial

membrane and is most highly expressed throughout the entire brain, in both neurons and glial cells (48, 64).

AGPAT5 is localized to the endoplasmic reticulum, nuclear envelope, and the mitochondria, with highest tissue expression in the testes (62). It shows similar substrate preference to AGPAT3, with a preference for oleoyl-CoA (18:1) over arachidonoyl-CoA, except that AGPAT5 utilizes lysophosphatidylethanolamine (LPE) as a fatty acyl acceptor, in addition to LPA, LPC, LPS, and LPI (62).

AGPAT6-11 have been shown to have AGPAT activity, catalyzing the acylation of LPA to PA. However, these enzymes have been shown to have much higher activity using other lysophospholipid substrates, and have been renamed for their other activities (44, 45, 55-58). AGPAT6 was first designated as LPAATζ but was shown to have predominant activity towards G3P instead of LPA and thus, is a microsomal GPAT that was renamed GPAT4 (45, 49). AGPAT7 was first discovered as an LPA acyltransferase localized to the endoplasmic reticulum, but was later shown to have predominant acyltransferase activity towards LPE (50). AGPAT7 was therefore renamed acyl-CoA:lysophoshatidylethanolamine 2 (LPEAT2) and was found to have highest expression in the brain, with a broad preference for longer fatty acyl chain donors, such as C16:0, C18:0, C18:1, but no preference for the degree of saturation (55). AGPAT8 was originally discovered as acyl-CoA:lysocardiolipin acyltransferase 1 (ALCAT1), an enzyme localized to the mitochondria-associated membrane (MAM) showing activity with monolysocardiolipin (MLCL) and dilysocardiolipin (DLCL) as fatty acyl acceptors and linoleoyl-CoA (C18:3n-3) and oleoyl-CoA (18:1n-9) as acyl donors (56, 65). ALCAT1 also has activity towards LPA, although relatively low, and a preference for C16:0 and C18:0 fatty acyl-CoA donors, and was found to have highest expression in the heart (51). AGPAT9 was found to catalyze the acylation of LPC to PC as well as the formation of PA from LPA, albeit at low levels, and was therefore renamed acyl-CoA:lysophosphatidylcholine acyltransferase 1 (LPCAT1) (52, 57). AGPAT9/LPCAT1 is localized to the endoplasmic reticulum and is highly expressed in the lung, in alveolar type II cells in particular, and in the spleen (52, 57). It prefers 18:1 as its major fatty acyl-CoA donor species (52). AGPAT10 was first identified as GPAT3 due to its high G3P acylation activities (44). However, it was later shown to also have activity towards the acylation of LPA, using 18:1 as the acyl donor. AGPAT10/GPAT3 localizes to the endoplasmic reticulum and shows highest expression in adipose tissue followed by the testis and kidney (44). AGPAT11 was first discovered as both acetyl-CoA:lyso-platelet-activating factor acetyltransferase (LysoPAFAT), due to its ability to produce

platelet-activating factor (PAF), and LPCAT2, due to its acyltransferase activity towards LPC and high sequence homology towards LPCAT1 (58). When AGPAT11 was cloned, it was found to have the same mRNA coding sequence as LPCAT2/lysoPAFAT, and to preferentially acylate LPA using 18:1-CoA. AGPAT11 localizes to the endoplasmic reticulum and is highly expressed in the lung, spleen and in leukocytes (53).

Table 1. Summary of the AGPAT isoforms

Isoform	Preferred lysophospholipid acceptor	Subcellular expression	Fatty acyl-CoA donor	Tissue Expression
1	LPA	ER	C18:1-CoA C18:2-CoA C15:0-CoA	Testis, pancreas, adipose tissue
2	LPA	ER	C18:1-CoA	Adipose tissue, pancreas, liver
3	LPA, LPC/LPI/LPS	ER Nuclear envelope Golgi apparatus	C18:1-CoA C20:4-CoA	Testis, pancreas, kidney
4	LPA	Mitochondria	C18:1-CoA	Brain, heart, adipose tissue
5	LPA, LPC/LPI/LPS/LPE	ER Mitochondria Nuclear envelope	C18:1-CoA	Testis, prostate
6 (GPAT4)	G3P	ER	C16:0-CoA C18:1-CoA	BAT, Mammary epithelium
7 (LPEAT2)	LPE	ER	C16:0-CoA C18:1-CoA	Brain
8 (ALCAT1)	MLCL, DLCL	MAM	C18:1-CoA C18:3-CoA	Heart
9 (LPCAT1)	LPC	ER	C18:1-CoA	Lung, spleen
10 (GPAT3)	G3P	ER	C18:1-CoA	Adipose tissue, testes, kidney
11 (LPCAT2)	LPC	ER	C18:1-CoA	Lung, spleen, kidney

AGPATs and GPATs in white adipose tissue

Several GPATs and AGPATs are known to be expressed in white adipose tissue and have been linked to the regulation of TAG production, to the differentiation of adipocytes, and to modulation of various pathologies including lipodystrophy, diabetes, and hepatic steatosis. In particular, GPAT3, GPAT4/AGPAT6, and AGPAT2 are all highly expressed in white adipose tissue and have been studied in either overexpression or gene ablation models in this tissue (41, 66-69).

GPAT3 has been suggested to be the predominant GPAT in differentiated 3T3-L1 cells and in WAT (41, 66). GPAT3 mRNA increased 60-fold during 3T3-L1 differentiation into mature adipocytes and was shown to function in the TAG biosynthesis branch of the Kennedy pathway, since overexpression of GPAT3 in HEK293 cells leads to increased incorporation of radiolabelled oleic acid into TAG, but not phospholipids, compared to controls (41). In *Gpat3*$^{-/-}$ mice, total GPAT activity in WAT was reduced by 80% compared to wildtype controls, and when fed a high fat diet, GPAT3-deficient mice showed lower body weights and reduced adiposity, increased energy expenditure, enlarged livers, and higher free cholesterol, cholesteryl esters, and TAG in the liver, suggesting that a lack of GPAT3 may impair the ability to store excess energy in adipose tissues (66).

GPAT4/AGPAT6 has also been shown to play a critical physiological role in the accumulation of TAG in white adipose tissue. *Gpat4/Agpat6*$^{-/-}$ mice show reduced body weight and TAG content, small gonadal WAT adipocyte size, and subcutaneous lipodystrophy (67). *Gpat4/Agpat6*-deficient mice were also shown to be resistant to both diet-induced and genetically-induced obesity, as seen by the maintenance of lower body weights when these animals were fed a high fat diet or were crossed onto the genetically obese leptin-deficient *ob/ob* background (67).

The role of AGPAT2 in the production and regulation of TAG synthesis was discovered originally from studies in patients with AGPAT2 mutations. These individuals have a form of congenital generalized lipodystrophy (CGL), also known as Berardinelli-Seip syndrome, which is an autosomal recessive disorder characterized by a lack of adipose tissue, insulin resistance, hypertriglyceridemia, hepatic steatosis, and early onset of diabetes (68). Although the exact mechanism by which AGPAT2 mutations cause lipodystrophy has yet to be elucidated, AGPAT2 has been shown to be imperative for both lipogenesis and adipogenesis. *Agpat2* is upregulated 40-fold during adipocyte differentiation and *Agpat2* knockdown results in delayed adipocyte differentiation and impaired TAG synthesis and storage (69). These findings indicate the importance of several

GPAT/AGPAT family members in adipocyte differentiation, TAG synthesis, and TAG storage. At present however, understanding of the role of AGPATs in adipose tissue biology is far from complete. Evidence indicates expression of other AGPATs in white adipose tissue, likely suggesting a functional role for additional AGPATs in maintaining healthy white adipose tissue and in modulating adipocyte-regulated metabolic disease.

Chapter 3: Rationale, Objectives, and Hypotheses

Rationale

The role of *Agpat4 in vivo* has yet to be fully determined. To date, three studies have published on the *in vitro* characterization of AGPAT4. Lu *et al*. (2005) showed that recombinant murine AGPAT4 synthesized in rabbit reticulocyte lysates had AGPAT activity, as measured by the amount of PA produced, although no AGPAT activity was observed in COS-1 cells transfected with the mammalian expression vector pcDNA3.1-mAGPAT4 (18). Eto *et al.* (2014) measured the lysophosphatidic acid acyltransferase capabilities of AGPAT4 in the microsomal fractions of Chinese hamster ovary (CHO)-K1 cells overexpressing the enzyme and found that it had AGPAT capabilities, preferentially esterifying LPA with long chain polyunsaturated fatty acids, especially docosahexaenoic acid (DHA, 22:6n-3) (70). Recently, Bradley *et al*. (2015) clarified prior ambiguous findings on AGPAT4 in a series of studies on the *in vitro* and *in vivo* role of this enzyme. Assays conducted in lysates from Sf9 cells infected with baculoviral *Agpat4* confirmed that AGPAT4 has *in vitro* acyltransferase activities towards LPA as an acyl acceptor, but not towards LPC, LPE, LPS, LPG, LPI, MLCL, or DLCL. Overexpression of AGPAT4 in Sf9 cells increased the endogenous cellular PI content by 72% compared to controls. In mice, *Agpat4* ablation significantly decreased the brain content of PI by 52%, PC by 39%, and PE by 32% compared to *wildtype* littermates, without changing PA, PS, PG or CL content (48). Interestingly, the levels of PA in the brains of the *Agpat4*$^{-/-}$ mice were identical to their *wildtype* littermates due to a compensatory upregulation of the other AGPAT homologs (1-5), but this was not sufficient to normalize downstream phospholipid synthesis. This indicated that the production of PA from LPA, as catalyzed by AGPAT4 in the brain, is shunted into specific downstream Kennedy pathway derivatives for the production of brain PC, PE, and PI and, therefore, AGPAT4 is an indirect, but essential, regulator of these phospholipids in the brain (48). Although *Agpat4* is most highly expressed in the brain, it does show substantial expression in both the heart and in perirenal WAT as well (Fig. 2).

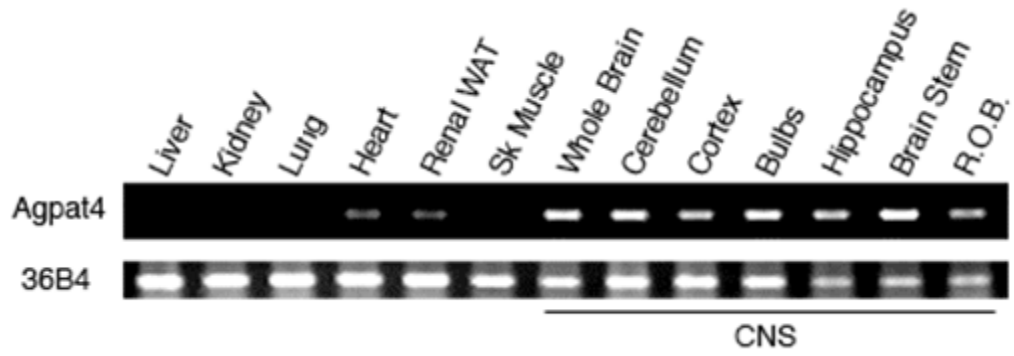

Figure 2. *Agpat4* expression in murine tissues. Real-time (RT)-PCR showing murine Agpat4 expression in various tissues and subsections of the central nervous system (CNS). R.O.B. = rest of brain.

The role of AGPAT4 in white adipose tissue has yet to be experimentally determined. We proposed to characterize the role of AGPAT4 in white adipose tissue using a gene ablation model where three major white adipose tissue regulatory processes were studied: adipogenesis, lipogenesis, and lipolysis.

Objectives

The primary objectives of this thesis were to characterize the *in vivo* biochemical and physiological role of AGPAT4 in the formation and maintenance of white adipose tissue. Using a gene ablation model of *Agpat4*, measures of whole body physiology, including measures of food intake, activity and energy metabolism, were determined. The epididymal and perirenal WAT depots were also assessed for weight and morphology as well as mRNA and protein expression of various adipogenic, lipolytic, and glycerolipid synthesis and remodeling genes, as well as lipolytic and lipogenic activities.

The first objective was to characterize the expression of AGPAT4 in various adipose tissue depots. Specific WAT depots, including epididymal, perirenal, retroperitoneal, and inguinal, as well as the subscapular brown adipose tissue (BAT) depot, from C57Bl/6J mice, were assessed for AGPAT4 mRNA expression relative to a loading control. Expression of *Agpat4* was also measured in the *wildtype* and *knockout* mice of the epididymal and perirenal white adipose depots to confirm the absence of *Agpat4* in the *Agpat4*$^{-/-}$ mice.

The second objective was to determine the effect of loss of AGPAT4 on adipose tissue depot masses and whole body physiology. This was determined by excision of specific adipose tissue depots at necropsy and by using the Comprehensive Laboratory Animal Monitoring System (CLAMS).

The third objective was to assess the role of AGPAT4 in the formation of phospholipids and TAG in epididymal and perirenal WAT. This was done by determining the quantity and composition of individual classes of phospholipids and TAG in epididymal and perirenal white adipose tissue depots using thin layer chromatography (TLC) followed by gas chromatography (GC).

The fourth objective was to assess the requirement for *Agpat4* in adipogenesis in both the epididymal and perirenal WAT depots. This was evaluated by determining mRNA expression of genes involved in the differentiation of adipocytes in *Agpat4*$^{-/-}$ mice as compared with *wildtype* mice. Furthermore, cell size was estimated from fixed sections of adipose depots.

The fifth objective was to determine the effect of *Agpat4* loss on lipogenesis in epididymal and perirenal WAT. This was done by assessing the mRNA of various lipogenic regulators as well as utilizing immunoblotting to measure the expression of various proteins involved in fatty acid synthesis in the epididymal and perirenal adipose depots of *Agpat*$^{-/-}$ and *wildtype* mice.

The sixth objective was to determine the effect of loss of *Agpat4* on the regulation of lipolysis in the epididymal and perirenal white adipose tissues. This was done through the assessment of protein expression of various lipolysis regulators in these depots. In addition, lipolytic activity was directly assessed using an *in vitro* radiochemical TAG hydrolysis assay with tissue extracts from *Agpat4*$^{-/-}$ and *wildtype* mice, and using an *in situ* assay in which fatty acid and glycerol release was measured from adipose tissue explants incubated in a physiological buffer.

The seventh objective was to measure the effect of loss of *Agpat4* on expression of other AGPAT isoforms (1, 2, 3, and 5*)* in both *wildtype* and *Agpat4*$^{-/-}$ mice to determine if compensation is observed.

Hypotheses

The hypotheses of this study are:

1. *Agpat4* expression will be ubiquitous amongst all white adipose tissue depots and will not be expressed in *Agpat4*$^{-/-}$ mice.
2. *Agpat4* ablation will result in a decrease in white adipose tissue masses, and whole body weights, as a result of reduced triacylglycerol synthesis.
3. *Agpat4* ablation will result in a decrease in the production of specific phospholipids, in epididymal and perirenal WAT, that may include PI, PC, and PE, and will also result in a decrease in TAG that is the major complex glycerolipid in adipose tissue.
4. *Agpat4* ablation will decrease differentiation in both the epididymal and perirenal adipose tissue depots, since TAG production is a critical signalling process in adipocyte differentiation, and TAG synthesis is expected to decrease in white adipose tissue.
5. *Agpat4* ablation will result in a decrease in lipogenesis in epididymal and perirenal WAT as AGPATs are responsible for the formation of PA, the branching point in which phospholipids and TAG are produced.
6. *Agpat4* ablation will result in a decrease in lipolytic activity as a compensatory mechanism in response to the expected decrease in TAG production and white adipose tissue mass.
7. *Agpat4* ablation will result in a compensatory induction of other *Agpats (1, 2, 3,* and *5)* in epididymal and perirenal WAT.

Chapter 4: Methods

Animals and Knockout Model

Adult male *Agpat4*$^{-/-}$ mice, aged 9 to 12 weeks old, were used with age-matched *wildtype* littermates as controls in all experiments. All mice were housed in a temperature and humidity controlled environment on a 12:12 hour reversed light/dark cycle and standard rodent chow and water were provided *ad libitum*. All animal procedures were approved by the University of Waterloo Animal Care Committee.

Heterozygous *Agpat4*$^{-/-}$ mouse embryos (B6;129S5-Agpat4^{tm1Lex}/Mmucd) were produced by Lexicon Genetics/Genentech through homologous recombination targeting coding exons 4, 5, and 6 out of the 9 *Agpat4* exons (NCBI accession NM_026644.1). The targeted mutation was generated in mouse 129S5/SvEvBrd embryonic stem cells with a LacZ/neomycin selection cassette and positive clones were identified by Southern blotting as previously reported (71). Progeny from clones 1A9 and 1P9 were crossed with C57BL/6J albino mice, generating F1 heterozygous animals, were cryorevived at the Mutant Mouse Regional Resource Center, and sent from the University of California at Davis to the University of Waterloo. Male and female heterozygous littermates were crossed to achieve F2 *wildtype*, *heterozygous* and *homozygous* mutant progeny. Mice used in experiments are produced by continuous backcrossing of heterozygotes.

DNA Isolation and Genotyping

DNA was isolated from ear punches after performing an overnight proteinase K digestion in which 400 µL of 1.0 mg/ml proteinase K in warmed lysis buffer (0.5% SDS, 0.1M NaCl, 0.05M Tris (pH 8.0), 2mM EDTA) was added to the ear punches and incubated at 63˚C for 24 hours. 75 µL of 8M potassium acetate and 500 µL of chloroform was added followed by vortexing at high speed for 5 to 10 minutes. The samples were centrifuged at 1,000 rpm for 5 minutes and the aqueous layer was retrieved. Two volumes of 100% ethanol were added, mixed through inversion, and centrifuged at 14,000 rpm for 20 minutes at 4˚C. The resulting pellet was air dried and eluted in water. DNA concentrations and purity were determined using a Nanodrop-2000 spectrophotometer (Thermo Scientific, Waltham, PA) and sample concentrations were subsequently adjusted to 250ng/µl.

Genotyping was determined by visualization of amplicons of the correct size in 1.0% agarose gels run in tris-acetate-EDTA (TAE) buffer following PCR amplification of DNA using primers specific for a region present only in the *wildtype* animals (located within intron 5) or primers specific to the recombined targeted region (crossing the end of the targeted sequence into the beginning of the

wildtype sequence in intron 6) (Fig. 3). PCR was performed using 1 μL of DNA with the following primers: *wildtype* (forward: 5'-TTA GCA TAG TGG GCG AAG TTC-3', reverse: 5'-GGT AGT GGC CAA GTT AAT AGT CCT-3'; 216 bp band produced only when the intact gene is present) and *Agpat4-/-* (forward: 5'-GCA GCG CAT CGC CTT CTA TC-3', reverse: 5'-CTC CCA TTT CTA GGA AGG AAG CAG-3'; 344 bp band produced only when *Agpat4* gene has been disrupted). Amplification was performed in a T100 Thermal Cycler (BioRad, Hercules, CA) with the following conditions: 94˚C for 5 minutes, 39 cycles of 94 ˚C for 1 minute, 58 ˚C for 1 minute, 72 ˚C for 30 seconds, followed by 72 ˚C for 10 minutes.

A

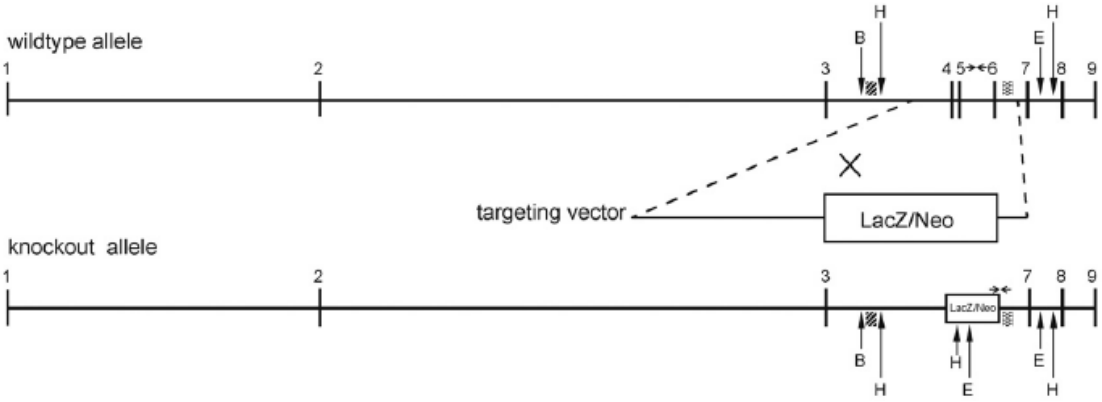

B

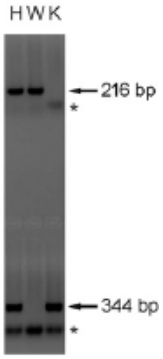

Figure 3. *Agpat4* gene ablation in mice. *A,* A LacZ/Neo fusion cassette replaced exons 4, 5, and 6, removing the catalytically critical EGTR motif in exon 5. Arrows indicate primers used for genotyping and letters indicate unique restriction sites where B = BgIII, H = HindIII, E = EcoRV site. *B,* Example genotyping analysis showing amplicon present only in wildtype mice (top) and amplicon present only in Agpat4$^{-/-}$ mice (top). W = wildtype, K = Agpat4$^{-/-}$, H = heterozygote.

Adipose tissue depot collection

Agpat4$^{-/-}$ and *wildtype* mice were euthanized via cervical dislocation, whole body weights were taken, and mice were placed in a dorsal position. An incision was made from the sternum to the pelvis in the sagittal plane and the gonadal white adipose depot in the lower pelvis, surrounding the reproductive organs and termed epididymal adipose tissue, was dissected out. The organs of the abdominal cavity were removed to expose the kidneys. The kidneys were excised and the white adipose tissue surrounding the organ, termed perirenal, was removed. The white adipose tissue in the abdominal cavity, dorsal to the kidneys and termed retroperitoneal, was then exposed and excised. A subcutaneous white adipose depot, termed inguinal, was excised by peeling away the skin in the hind region to expose the adipose tissue directly beneath the surface. Following, the mice were placed in a ventral position and the adipose tissue between the shoulder blades was dissected out. The white adipose tissue was removed from the sample, exposing the depot termed the subscapular BAT (Fig. 4). All tissues were immediately weighed and flash frozen in liquid nitrogen.

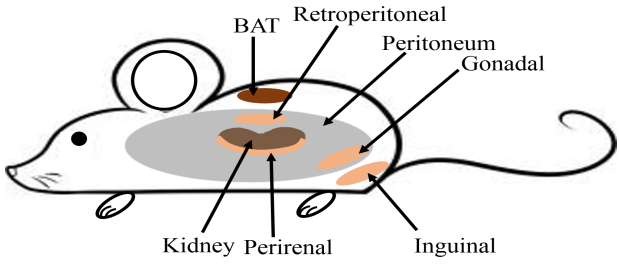

Figure 4. Excised adipose depot locations

Comprehensive Laboratory Animal Monitoring System (CLAMS)

An Oxymax Comprehensive Laboratory Animal Monitoring Systems (CLAMS) (Columbus Instruments, Columbus, OH) was used for two trials of 72 hours each. Oxymax is an open circuit indirect calorimeter used to determine Respiratory Exchange Ratio (RER), heat production, fat oxidation, carbohydrate oxidation, food consumption, total activity, dual beam movement, Z axis movement, daily average VO_2, and VO_2 while awake and sleeping. Animals were housed individually and a 2 hour acclimation period in the metabolic chamber occurred prior to monitoring over a 72 hour period under consistent environmental temperature (22˚C). RER was calculated using the ratio of carbon dioxide (VCO_2) to oxygen consumption (VO_2) and can indicate fat as the primary substrate (RER=0.7) or carbohydrate as the primary substrate (RER=1.0). Heat was determined using

the product of the calorific value (derived from the RER) and volume of oxygen consumed. Food consumption was determined by weighing the chow before and after measurements, and activity was determined through infra-red beam breaks.

RNA Isolation and Reverse Transcription (RT)-PCR

Total RNA was isolated from adipose tissues that were disrupted in TRIzol® reagent (Sigma-Aldrich, Oakville, ON) added at a concentration of 1 ml/≤100 mg, using a Polytron® homogenizer set at maximal velocity (VWR, Radnor, PA). Samples were then incubated at room temperature for an additional 5 minutes to ensure nucleoprotein complex dissociation. Chloroform (0.2 ml per mL of TRIzol® reagent used initially) was added and samples were vigorously shaken for 15 seconds, which was followed by incubation at room temperature for 2 minutes. Samples were centrifuged at 12,000 x *g* for 15 minutes at 4˚C. The upper aqueous phase, containing RNA, was added to a fresh tube and 0.5 mL of isopropanol was added per mL of TRIzol® reagent used initially. This was followed by incubation again at room temperature for 10 minutes to allow the RNA to precipitate. The samples were then centrifuged at 12,000 x *g* for 10 minutes at 4˚C to pellet the RNA. The supernatant was removed and the RNA pellet was washed using 1 mL of 75% ethanol per 1 mL of initial TRIzol® reagent. The samples were then vortexed and centrifuged at 7,500 *g* for 5 minutes at 4˚C. The ethanol was removed, the pellet was left to air dry at room temperature for 5-10 minutes and then re-suspended in 30 µl in deionized water. The solutions were incubated at 60˚C for 10 minutes to facilitate dissolution and subsequently stored at -80˚C.

Concentrations and purity of the RNA was determined using a Nanodrop-2000 spectrophotometer (Thermo Scientific) and RNA concentrations were adjusted to 2.5 µg/µl. Complementary DNA (cDNA) was generated through the reverse transcription of RNA using a Bio-Rad T100 Thermal Cycler. RNA was mixed with 4.2 µl double distilled H_2O (ddH_2O), 2 µl of 10x RT buffer, 0.8 µl 100 mM dNTPs, 2 µl 10x RT random primers, and 1 µl reverse transcriptase. Reverse transcription occurred at the following settings: 25˚C for 10 minutes, 37˚C for 2 hours, and 85 ˚C for 5 seconds. The cDNA was stored at -20 ˚C.

Quantitative PCR (qPCR) and Semi-quantitative PCR

Quantitative qPCR (qPCR) was performed using a Bio-Rad CFX96 Touch™ Real-Time PCR Detection System. cDNA was mixed with 1.5 µl ddH_2O, 7.5 µl SsoFast EvaGreen master mix (Bio-Rad), 0.5 µl of the forward primer and 0.5 µl of the reverse primer (25 pM final concentration). Amplification occurred with the conditions: 95˚C for 2 minutes, 40 cycles of 95˚C for 10 seconds,

60˚C for 20 seconds, followed by a melt curve to verify a single amplicon. The relative quantity of the gene of interest (ΔC_t) was calculated as ΔC_t=[C_t (gene of interest) - C_t (housekeeping gene)] with 18s used as the housekeeping gene for normalization. The relative expression of the gene of interest in the different white adipose depots ($\Delta\Delta C_t$) of the knockout animals was calculated relative to the same gene in the same depot in the *wildtype* animals as $\Delta\Delta C_t = \frac{2^{\Delta CT\ Gene-Knockout}}{2^{\Delta CT\ Gene-Wildtype}}$. Semi-quantitative PCR was performed in a T100 Thermal Cycler (Bio-Rad) with the following conditions: one cycle of 94˚C for 4 minutes, followed by 30 cycles of 94 ˚C for 30 seconds, 58 ˚C for 30 seconds, 72 ˚C for 1 minute, followed by a final extension of 72 ˚C for 10 minutes. 1 µl of cDNA was mixed with 2 µl of 10x buffer with $MgCl_2$, 0.4 µl of 10 mM dNTPs, 1 µl of the forward primer, and 1 µl of the reverse primer. Following PCR amplification, amplicons were resolved in a 1.0% TAE-agarose gel with ethidium bromide for visualization under ultraviolet light. Quantification occurred relative to the expression of 18S. All primers are listed in table 1.

Table 2. PCR primers

Gene	Direction	Sequence	Product Size
Agpat1	Forward	5'- AGA CCT TGC TCA CCC AGG AT-3'	134 bp
	Reverse	5' GAT GGG GAT GAT GGG GAC CT-3'	
Agpat2	Forward	5'-CCGTGGTGTACTCGTCTTTCT-3'	107 bp
	Reverse	5'-CAGACCATTGGTAGGGACAGC-3'	
Agpat3	Forward	5'-GCT TCG TCC TGG GTG TCT TT-3'	137 bp
	Reverse	5'-GTT GCC ATA GCT GGA GCC TT-3'	
Agpat5	Forward	5'-GGA CAT GTG CGC TAC GTA CT-3'	167 bp
	Reverse	5'-AGA TAC ATC GGT GTT CCT GCG-3'	
Atgl	Forward	5'-AACGCCACTCACATCTACGG-3'	113 bp
	Reverse	5'-GCCTCCTTGGACACCTCAATA-3'	
Cdipt	Forward	5'-GATCGACCTGTCTGGGAACC-3'	78 bp
	Reverse	5'-TTTCCAGCACACAGGGTGAA-3'	
Cds1	Forward	5'-TGGACATGGCGGGATAATGG-3'	111 bp
	Reverse	5'-TGGAGCACTTTGCTGGGATT-3'	
Cds2	Forward	5'-GGGTTCTTCGCCAGTGGATT-3'	89 bp
	Reverse	5'-AAGCGATCCATGATGCCTCC-3'	
C/ebpα	Forward	5'-GCAAAGCCAAGAAGTCGGTG-3'	114 bp
	Reverse	5'-TCTCCACGTTGCGTTGTTTG-3'	
C/ebpβ	Forward	5'-AAGCTGAGCGACGAGTACAAGA-3'	116 bp
	Reverse	5'-GTCAGCTCCAGCACCTTGTG-3'	
Cept1	Forward	5'-TTGTACTGTGGCAGGGACCA-3'	97 bp
	Reverse	5'-TGTTCCTGCTATGGTTGACCC-3'	
Chpt1	Forward	5'-ACTGTCTTTATTGGGCCAGGT-3'	90 bp
	Reverse	5'-GACCATTGCTATCCACAGAACA-3'	
Dgat1	Forward	5'-CTGGATTGTGGGCCGATTCT-3'	94 bp
	Reverse	5'-ATACATGAGCACAGCCACCG-3'	
Dgat2	Forward	5'-AAGACATCGACCTGTACCATGC-3'	92 bp
	Reverse	5'-CTCAGTCTCTGGAAGGCCAAA-3'	
Fabp4	Forward	5'-GTGGGATGGAAAGTCGACCA-3'	70 bp
	Reverse	5'-CATAACACATTCCACCACCAGC-3'	
Fat/cd36	Forward	5'-ACTGTGGCTAAATGAGACTGGG-3'	93 bp
	Reverse	5'-ACCATGCCAAGGAGCTTGAT-3'	
Hsl	Forward	5'-GGAGTCTATGCGCAGGAGTG-3'	80 bp
	Reverse	5'-GCTTCTTCAAGGTATCTGTGCC-3'	
Iplaβ	Forward	5'-CCTTTCCATTACGCTGTGCAA-3'	103 bp
	Reverse	5'-GACTCACGGCTTGGTTGTT-3'	
Iplaγ	Forward	5'-CAAAGACAAGAAGGCAGAGGAG-3'	106 bp
	Reverse	5'-TAAGGCCTGAACTAAGGCTCG-3'	
Lipin1	Forward	5'-CCTTAGGGAGCCGGAAGACT-3'	91 bp
	Reverse	5'-ATTGTTGGCGACTGGTCACT-3'	
Pgs1	Forward	5'-GGGTCCAGCTCCAGGAATAC-3'	111 bp
	Reverse	5'-TAGGAGAGCCAATCAGCGTG-3'	
Pka	Forward	5'-AATCGTCTCTGGGAAGGTGC-3'	118 bp
	Reverse	5'-GACCCCGTTCTTGAGGTTCC-3'	
Pparγ	Forward	5'-CACAATGCCATCAGGTTTGG-3'	82 bp
	Reverse	5'-GCTGGTCGATATCACTGGAGATC-3'	
Pref1	Forward	5'-GACAGGCCATCTGCTTCACC-3'	116 bp
	Reverse	5'-GTTGTAGCGCAGGTTGGACA-3'	
18s	Forward	5'-GATCCATTGGAGGGCAAGTCT-3'	79 bp
	Reverse	5'-AACTGCAGCAACTTTAATATACGCTATT-3'	

Paraffin Embedding and Hematoxylin and Eosin (H&E) Staining

White adipose tissue depots were collected from *Agpat4*$^{-/-}$ and *wildtype* control mice and embedded in paraffin. Briefly, fresh tissues were fixed in 4% paraformaldehyde for 48 hours at 4˚C and subsequently placed in embedding cassettes. Dehydration followed in which the cassettes, containing the samples, were washed with 70% ethanol twice for 1 hour each, with 80% ethanol twice for 1 hour each, 95% ethanol twice for 1 hour each, 100% ethanol 3 times for 1 hour each, and xylene three times for 1 hour each. The cassettes were then placed in paraffin wax for 1 hour, followed by an overnight incubation in a fresh change of paraffin wax, and another 1 hour incubation in fresh paraffin before embedding in paraffin blocks. Following embedding, the samples were cut into 6μm sections using a microtome and carefully transferred onto microscope slides where they were incubated overnight at 40˚C to facilitate adherence to the slide. Sample rehydration occurred next, where slides were washed with xylenes 3 times for 5 minutes, 100% ethanol 2 times for 2 minutes, 95% ethanol for 1 minute, 70% ethanol for 1 minute, and running water for 1 minute. Hematoxylin was then added and left on the slides for 3 minutes, followed by a 1 minute wash in running water, incubation in Scott's solution (5g $MgSO_4$, 0.33g Na_2CO_3, 500ml tap water) for 1 minute, a 1 minute wash in running water again, 80% ethanol for 1 minute, and then 95% ethanol for 1 minute. Eosin was added and left on the slides for 3 minutes, followed by a brief 95% ethanol wash, 100% ethanol 3 times for 1 minute, and 3 changes of xylene for 2 minutes. Microscope slides were then be imaged and cross-sectional areas quantified using Image J software (72). Five separate fields from four different mice were quantified.

Protein Extraction and Immunoblotting

White adipose tissue depots were collected from *Agpat4*$^{-/-}$ mice and homogenized on ice in lysis buffer (50 mM Tris, pH 7.4, 1 mM EDTA, 0.1 M sucrose, 5mM sodium fluoride, 10 mM sodium orthovanadate, with protease inhibitor cocktail (1:100)) using a Polytron® homogenizer (VWR). Centrifugation occurred at 10,000 x *g* for 10 minutes at 4˚C and the supernatant was collected and sonicated on ice at 65 amp for 6 seconds, 3 times. Protein concentration was determined using a bicinchoninic acid (BCA) assay in which 100 μl of 4% copper sulfate in BCA 1:50 was added to 5 μl of protein sample followed by incubation at 37˚C for 30 minutes. Absorbance was measured at 527 nm. Protein concentration was determined using a bovine serum albumin (BSA) standard curve.

Equivalent masses of total protein were mixed with 6X protein loading dye (375 nM Tris HCl, 9% SDS, 50% glycerol, 0.03% bromophenol blue) and heated for 5 minutes at 95˚C. Samples

were electrophoresed through Bio-Rad 10% TGX Stain-Free FastCast Acrylamide gels at 200 V for 30 minutes, followed by a transfer onto a nitrocellulose membrane at 0.35A for 90 minutes. Blocking was performed using a 3% blocker (w/v) in TBST (50 mM Tris-HCl, pH 7.4, 150 mM NaCl, 0.1% Tween-20) for 1 hour. The nitrocellulose membranes were then incubated at 4˚C overnight with a primary antibody, at 1:1000 in 3% blocker (w/v) in TBST, against the protein of interest. The following antibodies, purchased from cell signaling (Beverly, MA), were used: ATGL, HSL, phosphorylated (P)-HSL S563, P-HSL S565, P-HSL S660, perilipin, AMPK α, acetyl-CoA carboxylase (ACC), P-ACC S79, and FAS. The membranes were washed 3 times for 15 minutes in TBST and incubated for 1 hour with a horseradish peroxidase (HRP)-conjugated secondary antibody in TBST with 3% blocker (w/v). The membranes were washed 3 times for 15 minutes followed by the addition of Luminata™ Crescendo HRP substrate chemiluminescence reagent. Imaging occurred using a Bio-Rad ChemiDoc™ Touch Imaging system and the size of proteins of interest were determined using a Bio-Rad precision plus protein™ standard with a 10-200 kDa wide range. Equal protein loading was determined through quantification of total protein by imaging a stain-free gel to determine total protein content per lane. Skim milk powder was used as a blocker for ATGL and BSA was used as a blocker for the remainder of the proteins.

Extraction of Adipose Tissue Lipids and Lipid Analysis

White adipose tissue depots were collected from *Agpat4*$^{-/-}$ mice and total lipids were extracted as described by Folch *et al*., in 1957 (73). 50 mg samples were homogenized in glass tubes in 2:1 (v/v) chloroform:methanol using a Polytron® homogenizer (VWR) and 500 µl of sodium phosphate was added, followed by 3x inversion and centrifugation at 3,000 rpm for 5 minutes. The organic layer was collected and 2 ml of chloroform was added to the remaining layers, and this was followed by centrifugation at 3,000 rpm for 5 minutes and a second collection of the organic layer. The organic layers were pooled, dried with nitrogen gas to reduce the volume, and then applied to a silica gel G plate (Analtech, Newark, NJ) with a solvent front containing hexane:diethyl ether:glacial acetic acid (80:20:2, v/v/v) for neutral lipid separation by thin layer chromatography. Bands were visualized by spraying the plates with 2',7'-dichlorofluorescein. The band corresponding to TAG, as determined by comparison to a known TAG standard, was scraped for analysis of fatty acid content and composition by gas chromatography. The band corresponding to polar lipids, remaining at the origin, was also scraped, followed by lipid extraction. The resulting organic layer was dried with nitrogen gas to reduce the volume and applied to a silica H plate (Analtech) that was then resolved using a solvent mixture of chloroform:methanol:isopropanol:0.25% KCL:triethylamine (30:9:25:6:18,

v/v/v/v/v) to separate individual phospholipid classes. The bands corresponding to these phospholipid classes were identified using known standards (Avanti Polar Lipids, Alabaster, AL) and scraped. The total lipid extraction procedure was performed with the addition of an internal standard (10 μg 22:3n-3 methyl ester per ml of 2:1 chloroform:methanol) in order to estimate recovery and an antioxidant was added to prevent destruction of unsaturated fatty acids (50 μg/ml BHT). Gas chromatography with flame ionization detection was performed to determine the fatty acid composition of each class of phospholipids as described by Metherel *et al.* in 2009 (74). These values were also used to estimate the total concentration of each phospholipid within the tissue. Briefly, transesterification using 14% boron trifluoride in methanol (Thermo Fisher Scientific) occurred with hexane on a 95˚C heat block for 1 hour to convert lipid fatty acyl chains into fatty acid methyl esters. Analysis was then performed using a Varian 3900 gas chromatograph equipped with a DB-FFAP 15m x 0.1mm injected dose x 0.10μm film thickness, nitroterephthalic acid modified, polyethylene glycol, capillary column (J&W Scientific from Agilent Technologies, Mississauga, ON) with hydrogen as the gas carrier. A volume of 1 μl of each sample was introduced by a Varian CP-8400 autosampler into the injector heated to 250˚C with a split ratio of 200:1. The temperature began at 150˚C with a 0.25 min hold which was followed by a 35˚C/min ramp to 200 ˚C, an 8˚C /min ramp to 225˚C with a 3.2 min hold and finally, an 80˚C/min ramp up to 245˚C with a 15 min hold. The temperature of the flame ionization detector was 300˚C with air and nitrogen make-up gas flow rates of 300 and 25 mL/ min, respectively, and a sampling frequency of 50 Hz. An external reference standard (GLC-462, Nu Chek Prep, Elysian, MN) was used to identify individual fatty acid peaks.

Radiochemical in vitro triolein hydrolase assay

Protein lysates containing 100 μg of protein in 100 μl of lysis buffer were added to 100 μl of a reaction mixture containing 300 μM triolein with [9,10-^{3}H(N)]triolein (0.15 μCi per reaction), 25 μM egg yolk lecithin, 2% BSA (w/v), 100 μM sodium taurocholate, 50 mM potassium phosphate (pH 7.2), and 1 mM DTT. The reaction mixture was incubated at 37˚C for 1 hour and quenched by the addition of 0.25 ml of 2:1 chloroform:methanol. Total lipid extraction occurred using the method as described by Bligh and Dyer in 1959 (75). Briefly, 0.250 ml of chloroform was added to the quenched mixture, followed by vortexing for 30 seconds, the addition of 0.250 ml ddH_2O, vortexing for 30 seconds, and centrifugation for 5 minutes at 1000 x *g*. The organic phase was retrieved, dried with nitrogen gas, and applied to a silica gel G plate with a solvent front containing hexane:diethyl ether: glacial acetic acid (80:20:2, v/v/v) for neutral lipid separation. The band corresponding to non-

esterified fatty acids (NEFA), as determined by known standards, was scraped and subject to liquid scintillation counting for quantification of hydrolyzed fatty acids.

In situ lipolysis assay

Epididymal and perirenal WAT explants were assayed for glycerol and free fatty acid release, as previously described (76). Briefly, 50 mg samples of tissue from overnight-fasted mice were excised and incubated immediately in 500 µl of Krebs-Ringer solution (0.12 M NaCl, 4.7 mM KCl, 2.5 mM $CaCl_2$, 1.2 mM $MgSO_4$, 1.2 mM KH_2PO_4) with 20 mM HEPES, 2% fatty acid-free BSA, and 0.1% glucose. Aliquots were measured at time point 0, 30 minutes, 1 hour, 2 hours, and 4 hours, for fatty acid and glycerol release using a NEFA Reagent (Wako Diagnostics, Mountain View, CA) and Free Glycerol Reagent (Sigma-Aldrich), respectively.

Triacylglycerol and non-esterified fatty acids plasma assays

Blood samples were obtained from *Agpat4*$^{-/-}$ mice and their *wildtype* counterparts and spun at 1,000 x *g* for 10 minutes at 4˚C. The top layer, containing plasma, was obtained for analysis of TAG and NEFA content using a triglyceride colorimetric assay kit and free fatty acid fluorometric assay kit from Cayman chemicals (Ann Arbor, Mi), according to the manufacturer's instructions.

Statistical analysis

Mice were divided into two groups based on *Agpat4* expression (wildtype versus knockout). The results are shown as means ± SEM. Significance between the two groups was established using Student's *t*-test (unpaired, two-tailed) and significance between multiple groups was established by one-way analysis of variance with Bonferroni's post hoc test. Differences were considered significant at $P < 0.05$.

Chapter 5: Results

Agpat4 is expressed in adipose tissue

To confirm *Agpat4* expression in perirenal WAT, and determine if expression is depot specific, RT-PCR was utilized to visualize bands in an ethidium bromide gel (Fig. 5A) and quantified (Fig. 5B). Analysis indicated expression within each adipose tissue depot in C57Bl/6J mice without any statistically significant differences between the regions.

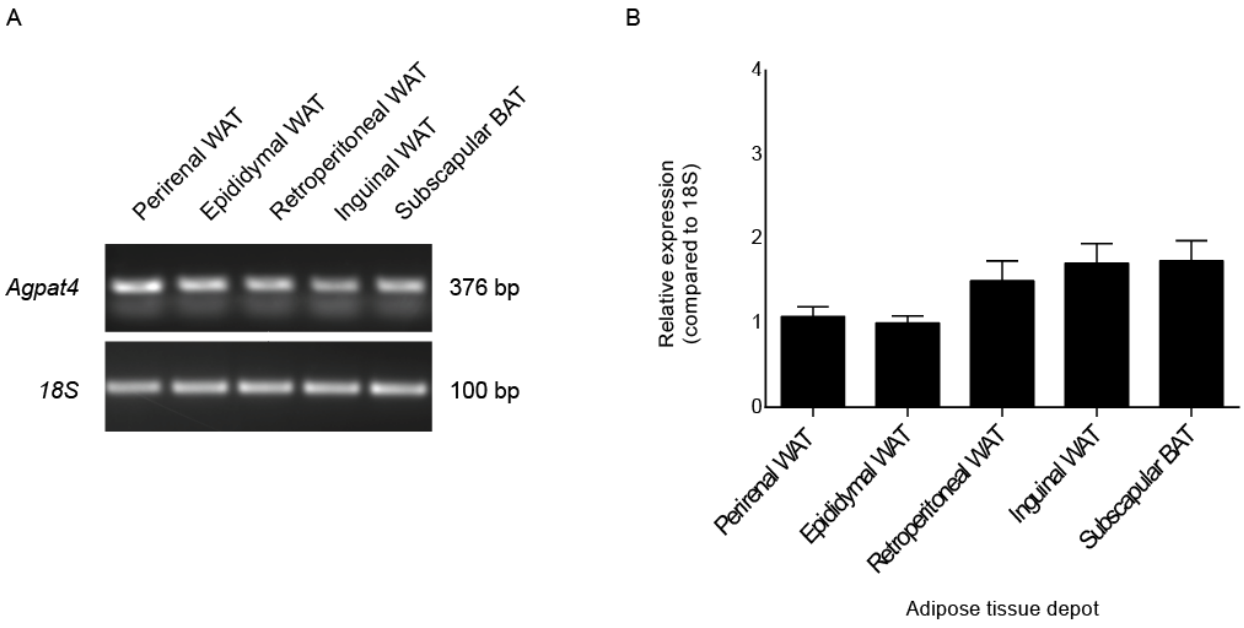

Figure 5. *Agpat4* expression in multiple adipose tissue depots in C57Bl/6J mice. *A*, Representative ethidium bromide gel showing murine *Agpat4* expression, as measured by RT-PCR, in various adipose depots, in C57Bl/6J mice. *B*, Quantification of AGPAT4 mRNA expression, as measured by RT-PCR, in various adipose depots. (n=3). Data are means ± SEM

Agpat4 gene ablation results in loss of Agpat4 expression in WAT

To determine the critical biochemical and physiological role of AGPAT4 in adipose tissue, an *Agpat4* gene ablation model was created. To confirm the absence of *Agpat4* expression in the adipose tissues analyzed in this dissertation, RT-PCR was utilized. The absence of a band corresponding to *Agpat4*, relative to *18S* expression, was confirmed in both epididymal (Fig. 6A) and perirenal (Fig. 6B) white adipose tissue.

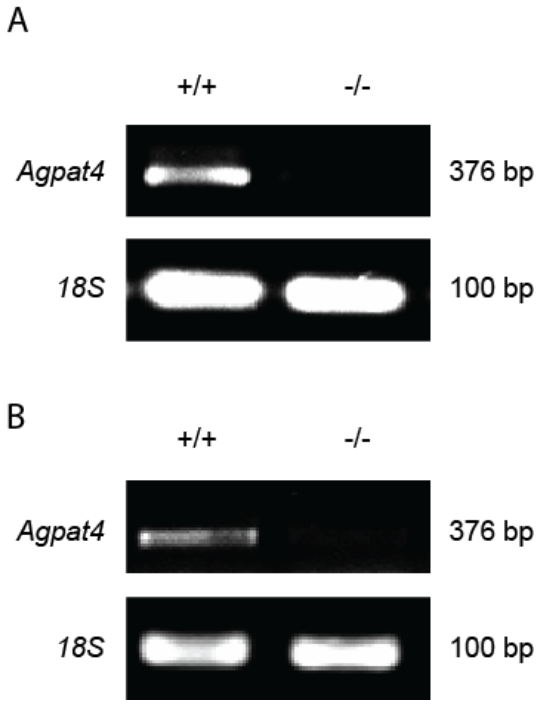

Figure 6. *Agpat4* expression in *wildtype* and *Agpat4*$^{-/-}$ mice. RT-PCR confirming the absence of *Agpat4* expression in *Agpat4*$^{-/-}$ mice in *A*, epididymal WAT and *B*, perirenal WAT. (n=3).

Epididymal WAT weight is higher in Agpat4$^{-/-}$ mice but whole body weights are not different

Whole body weights of *Agpat4*$^{-/-}$ and *wildtype* mice were recorded but no statistically significant differences were found (Fig. 7A). The weights of individual adipose tissue depots were also assessed and expressed as mg of tissue per g of body weight (Fig. 7B). No statistically significant differences were seen between *Agpat4*$^{-/-}$ and *wildtype* mice for the perirenal, retroperitoneal, or inguinal white adipose or the subscapular brown adipose depots. However, analysis indicated that the epididymal WAT depot in *Agpat4*$^{-/-}$ mice showed a 40% increase in weight compared to *wildtype* littermate controls (24.65 ± 2.00 versus 17.60 ± 1.46 mg tissue/g body weight, respectively, $P < 0.05$).

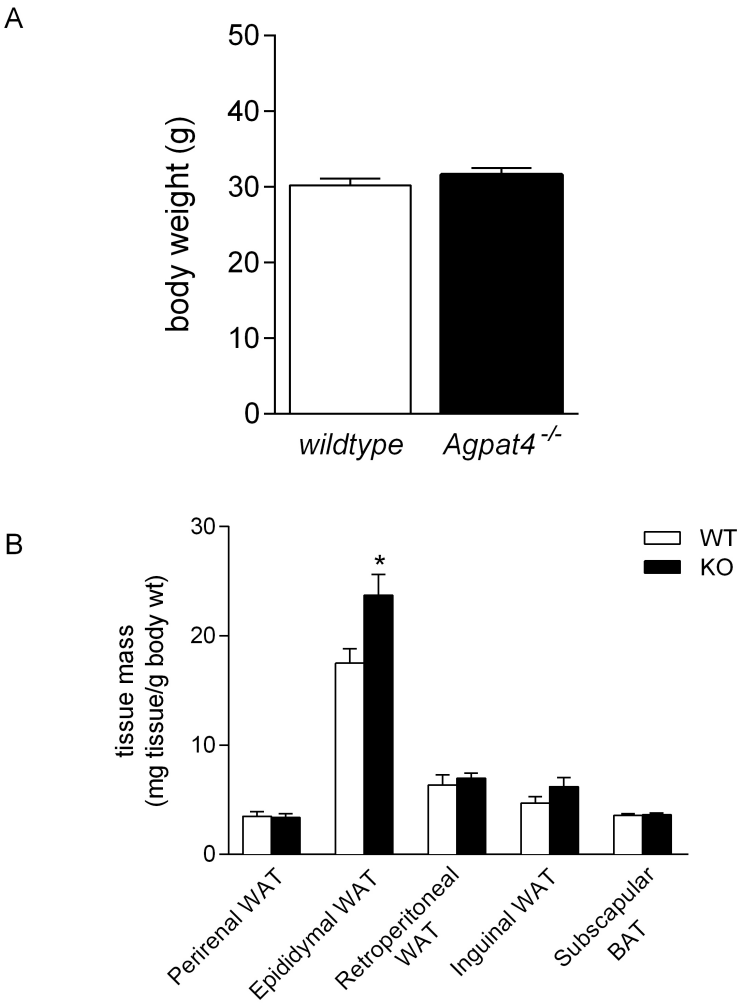

Figure 7. Body mass and adipose depot weight analysis. *A*, Mouse carcass mass as determined immediately after exsanguination at age 9-12 weeks (n=25-28). *B*, Adipose depot weights from *wildtype* and *Agpat4*$^{-/-}$ mice as expressed relative to whole body weight. (n=20-34). Data are means ± SEM. *$P < 0.05$ vs. *wildtype*.

Loss of Agpat4 does not alter food intake, activity, or energy metabolism

To determine if the greater epididymal WAT weight in *Agpat4*$^{-/-}$ is due to differences in dietary consumption, activity, or energy metabolism, CLAMS was used to assess food intake, total activity, dual beam movement, Z-axis movement, RER, heat expended, fat oxidation, carbohydrate oxidation, daily average VO_2, VO_2 awake, and VO_2 sleeping (Fig. 8). There were no significant differences measured during the 72 hour period, suggesting the difference in epididymal WAT weight is not due to differences in food intake, activity, or energy metabolism.

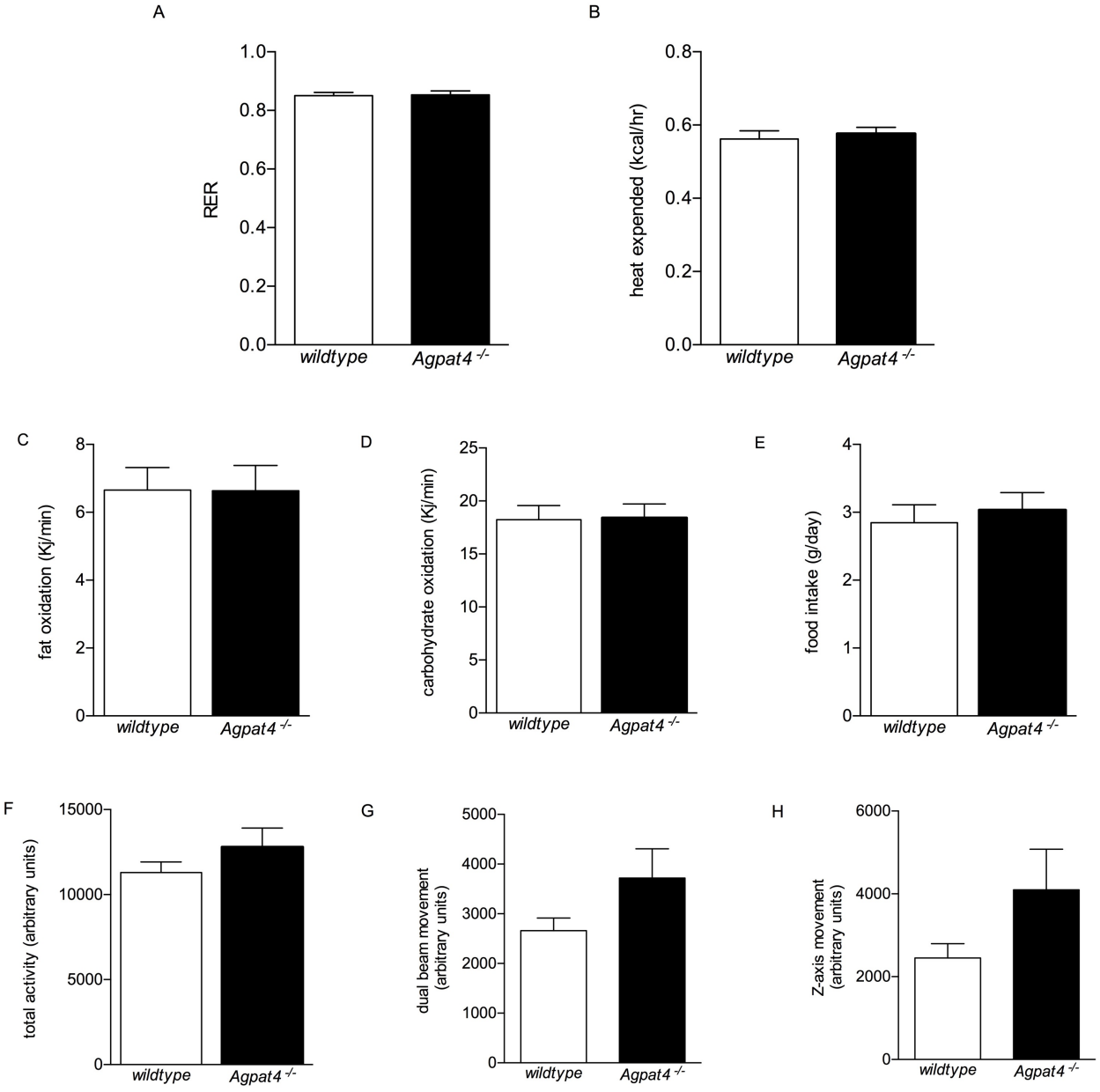

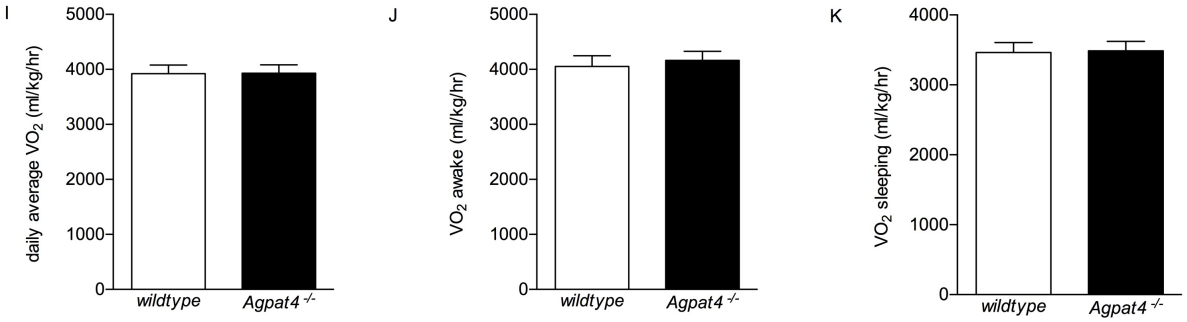

Figure 8. Measures of food intake, activity, and energy metabolism in *Agpat4*$^{-/-}$ and *wildtype* mice. Measures of whole body physiology, as determined through CLAMS. *A,* RER. *B*, heat expended. *C,* fat oxidation. *D,* carbohydrate oxidation. *E,* food intake. *F,* total activity. *G,* dual beam movement. *H,* Z-axis movement. *I,* daily average VO_2. *J,* VO_2 awake. *K,* VO_2 sleeping. (n=14-15). Data are means ± SEM.

TAG content is increased in the epididymal WAT of Agpat4$^{-/-}$ *mice*

Total lipid extracts were obtained from *Agpat4*$^{-/-}$ mice and their *wildtype* counterparts from epididymal WAT, to determine if an increase in TAG is resulting in the increase in epididymal WAT weights in the *Agpat4*$^{-/-}$ mice. Total lipid extracts were also taken from a second visceral depot, the perirenal WAT depot, for comparison. The lipid extracts from both depots were subjected to TLC to separate TAG for GC analysis and the results are expressed as μg of fatty acid per mg of tissue. Epididymal WAT from *Agpat4*$^{-/-}$ mice had a 26% significantly greater TAG content compared to *wildtype* mice (936.26 ± 52.75 versus 741.02 ± 21.61 μg FA/mg adipose tissue, respectively, $P < 0.05$) (Fig. 9A).This was accompanied by a significantly greater content of saturated fatty acids (SFA) in the TAG in *Agpat4*$^{-/-}$ mice (33% greater; 473.85 ± 32.91 versus 355.80 ± 30.99 μg SFA/mg epididymal adipose tissue, $P < 0.05$) (Fig. 9B) and a significantly greater content of monounsaturated fatty acid (MUFA) in the TAG in *Agpat4*$^{-/-}$ mice (392.06 ± 27.52 versus 321.14 ± 13.20 μg MUFA/mg epididymal adipose tissue, $P < 0.05$) (Fig. 9C). No significant differences were found between *wildtype* and *knockout* mice in the epididymal TAG n-6 (Fig. 9D) or n-3 (Fig. 9E) composition. In perirenal WAT, no significant differences in total TAG content or fatty acid composition were observed (Fig. 10).

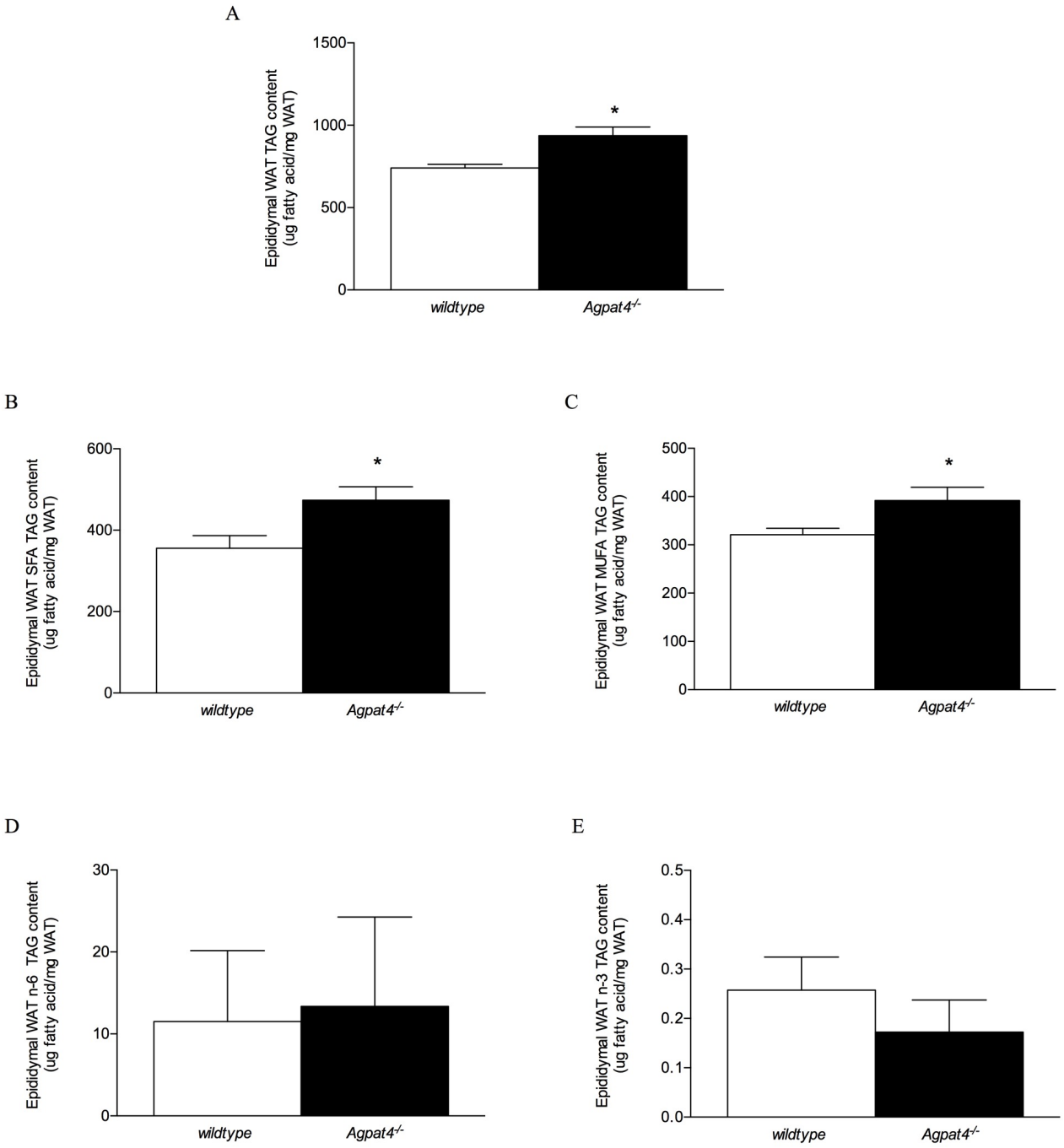

Figure 9. Triacylglycerol and fatty acid analysis of epididymal WAT. GC analysis of the total lipid extract of epididymal WAT in *Agpat4*$^{-/-}$ and *wildtype* mice. *A,* TAG concentration. *B,* TAG SFA content. *C*, TAG MUFA content. *D,* TAG n-6 polyunsaturated fatty acids (PUFA). *E,* TAG n-3 PUFA. (n=4). *P < 0.05 vs. *wildtype*.

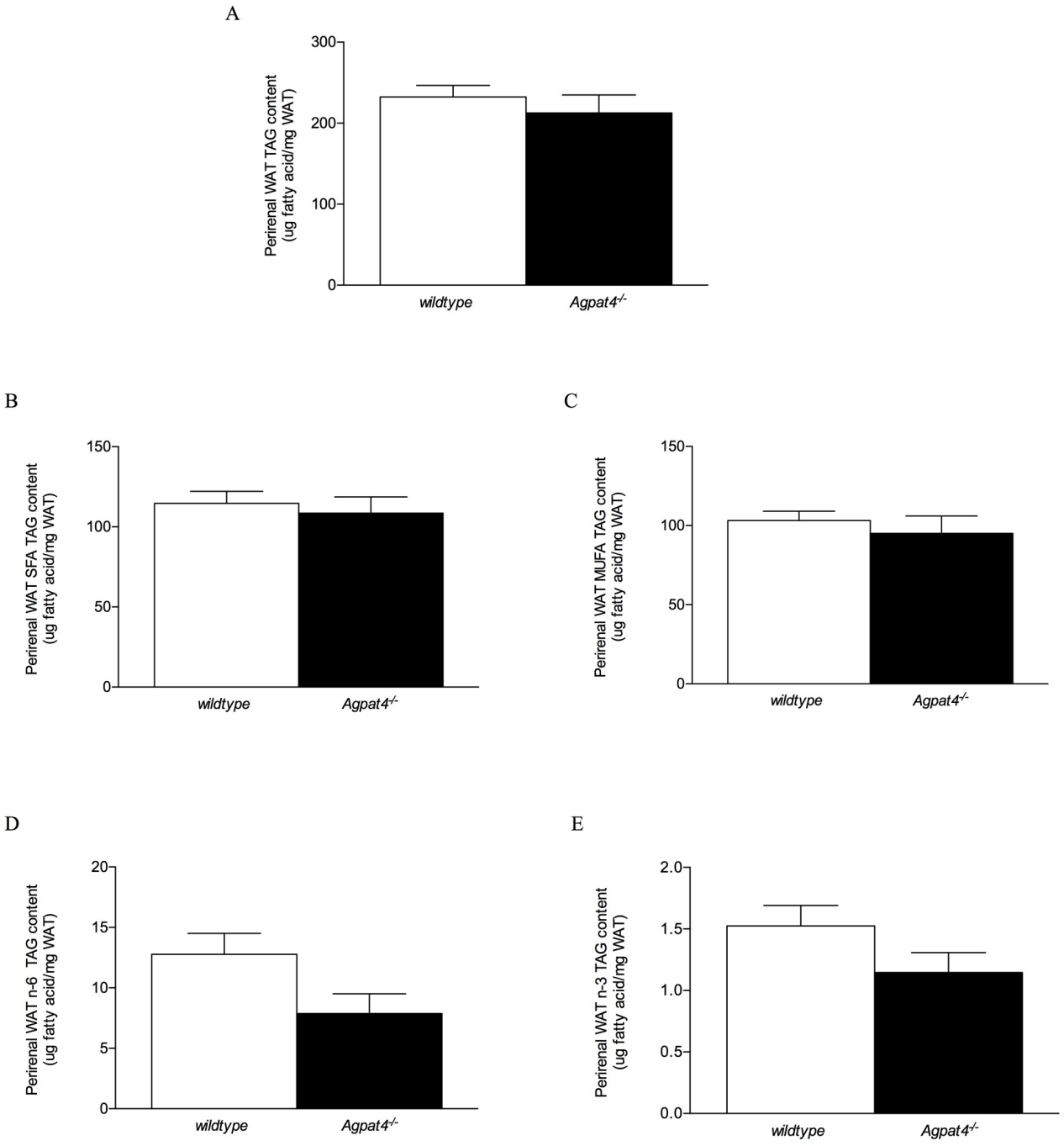

Figure 10. Triacylglycerol and fatty acid analysis of perirenal WAT. GC analysis of the total lipid extract of perirenal WAT in *Agpat4*$^{-/-}$ and *wildtype* mice. *A,* TAG concentration. *B,* TAG SFA content. *C*, TAG MUFA content. *D,* TAG n-6 PUFA. *E,* TAG n-3 PUFA. (n=5). Data are ± SEM.

PA content is increased in the epididymal WAT of Agpat4$^{-/-}$ mice

Previously, Bradley *et al.* (48) showed that the brains of *Agpat4*$^{-/-}$ mice have decreased PI, PE, and PC content. To determine if this decrease in specific phospholipids is tissue specific, or if the same changes are evident in adipose tissue as well, total lipid extracts of epididymal and perirenal WAT from *Agpat4*$^{-/-}$ and *wildtype* mice were subjected to polar lipid TLC separation, to resolve the individual classes of phospholipids, followed by GC analysis. The results are expressed as μg of fatty acid per g of tissue. Epididymal WAT from *Agpat4*$^{-/-}$ mice exhibited 74% greater total cellular PA content compared to *wildtype* mice (150.76 ± 25.97 versus 86.52 ± 8.71 μg FA/g adipose tissue, $P < 0.01$) but no significant differences were observed in the content of PC, PE, PI, PG, PS, or CL (Fig. 11A). In perirenal WAT, no significant differences were observed in the content of any of the measured phospholipids (Fig. 11B).

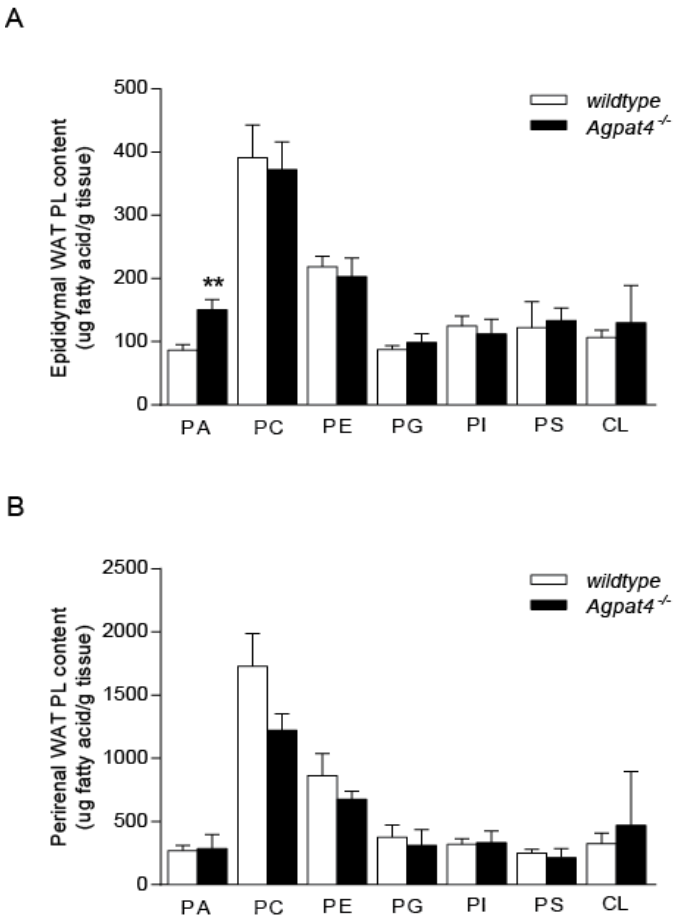

Figure 11. Phospholipid content of epididymal and perirenal WAT. Phospholipid content, as determined by GC analysis, of the total lipid extract of *A,* Epididymal WAT and *B,* Perirenal WAT of *Agpat4*$^{-/-}$ and *wildtype* mice. (n=4-5). Data are ± SEM. *P < 0.05 vs. *wildtype*.

Lipid droplet size, but not differentiation, is increased in the epididymal WAT of Agpat$^{-/-}$ mice

Increased WAT mass and subsequently, TAG content, can result from an increase in adipocyte number, due to increased adipogenesis, or from an increase in adipocyte size (77). To determine if the *Agpat4*$^{-/-}$ mice show increased adipogenesis in the epididymal WAT depot, expression was analyzed for genes encoding proteins involved in adipocyte differentiation using qPCR (Fig. 12A). The results were also compared to analysis of gene expression in the perirenal WAT depot (Fig. 12B). No significant differences were found in the expression of genes encoding C/EBPα, C/EBPβ, PREF-1, PPARγ, iPLAβ, iPLAγ, aP2/FABP4, or FAT/CD36 between *wildtype* and *Agpat4*$^{-/-}$ mice in either the epididymal or the perirenal WAT depot, suggesting that the degree of differentiation of these depots did not differ significantly between *wildtype and Agpat4*$^{-/-}$ mice, and that an increase in adipocyte size was more likely to be responsible for the increase in epididymal WAT mass.

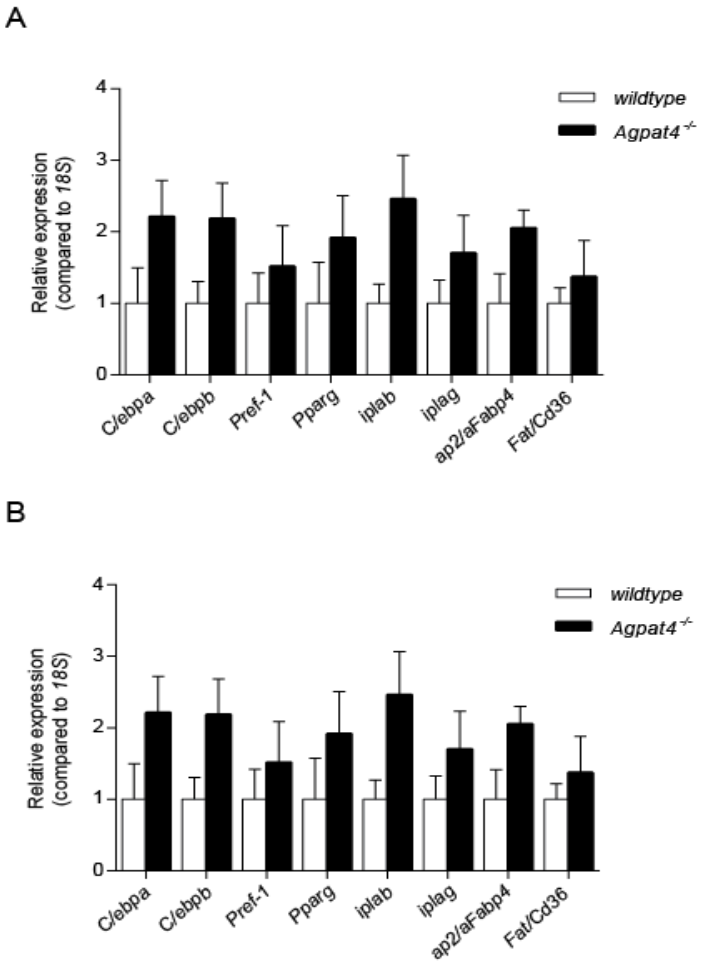

Figure 12. Adipogenic gene expression. Analysis of expression of genes encoding enzymes involved in adipocyte differentiation in *Agpat4*$^{-/-}$ *and wildtype* mice from *A,* epididymal WAT and *B,* perirenal WAT. (n=5-7). Data are means ± SEM.

To assess if adipocyte size increased, in accordance with the increase in epididymal WAT weight and TAG content in *Agpat4*$^{-/-}$ mice, epididymal WAT was sectioned and stained with hematoxylin and eosin (Fig. 13), and five separate fields were counted from four different mice. The results were compared with that of perirenal WAT (Fig. 14). Histological analysis indicated a greater frequency of large adipocytes in epididymal WAT of *Agpat4*$^{-/-}$ mice when compared to *wildtype* littermates as seen by the presence of significantly more adipocytes >1300 μm^2 in *Agpat4*$^{-/-}$ mice. The average adipocyte cell size was also significantly greater in *Agpat4*$^{-/-}$ mice. These differences were not see in perirenal WAT.

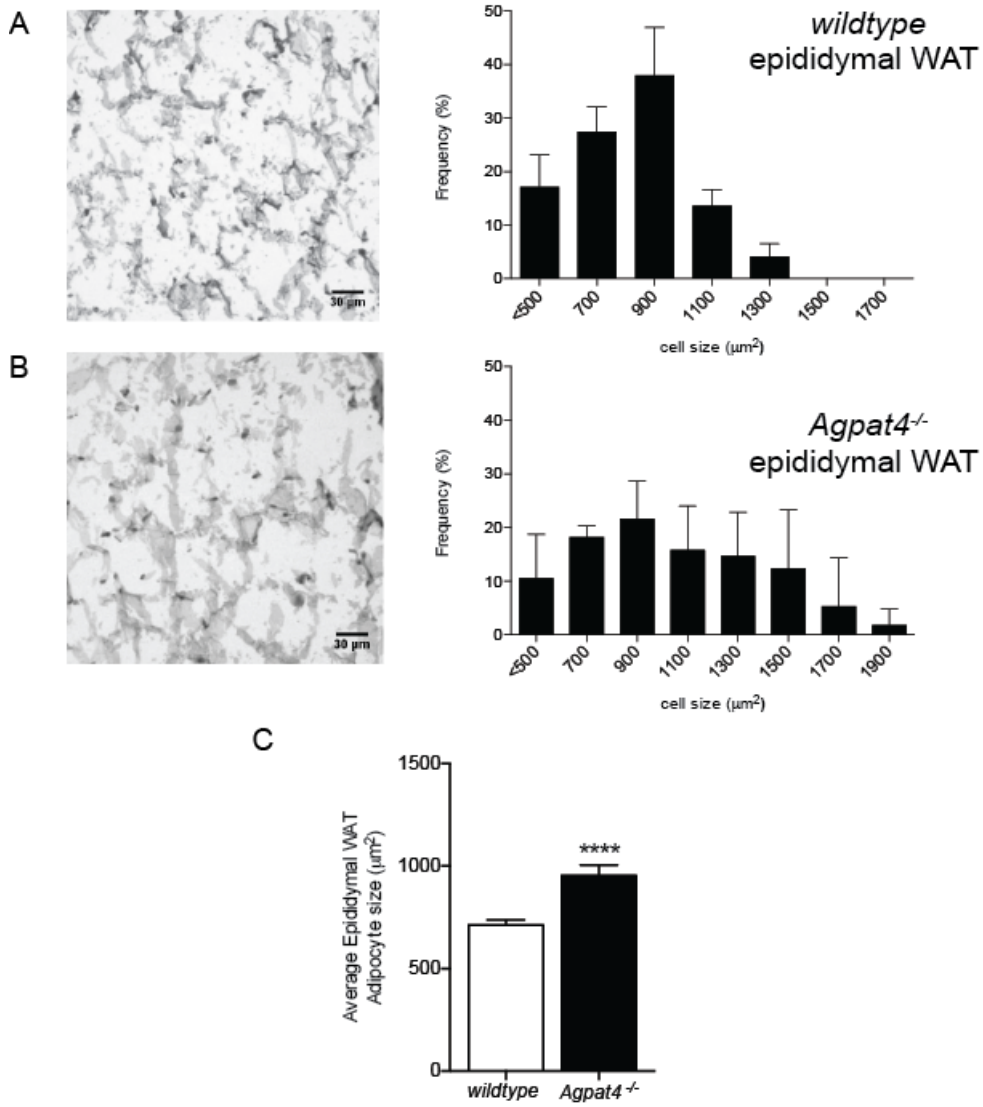

Figure 13. Adipocyte size in epididymal WAT. *A,* Representative image of *wildtype* hematoxylin & eosin-stained sections of epididymal WAT and frequency distribution of adipocyte cell size. *B,* Representative image of *Agpat4*$^{-/-}$ hematoxylin & eosin-stained sections of epididymal WAT and frequency distribution of adipocyte cell size. *C,* Average adipocyte cell size. (n=4). Data are means ± SEM. ****P < 0.0001 vs. *wildtype*.

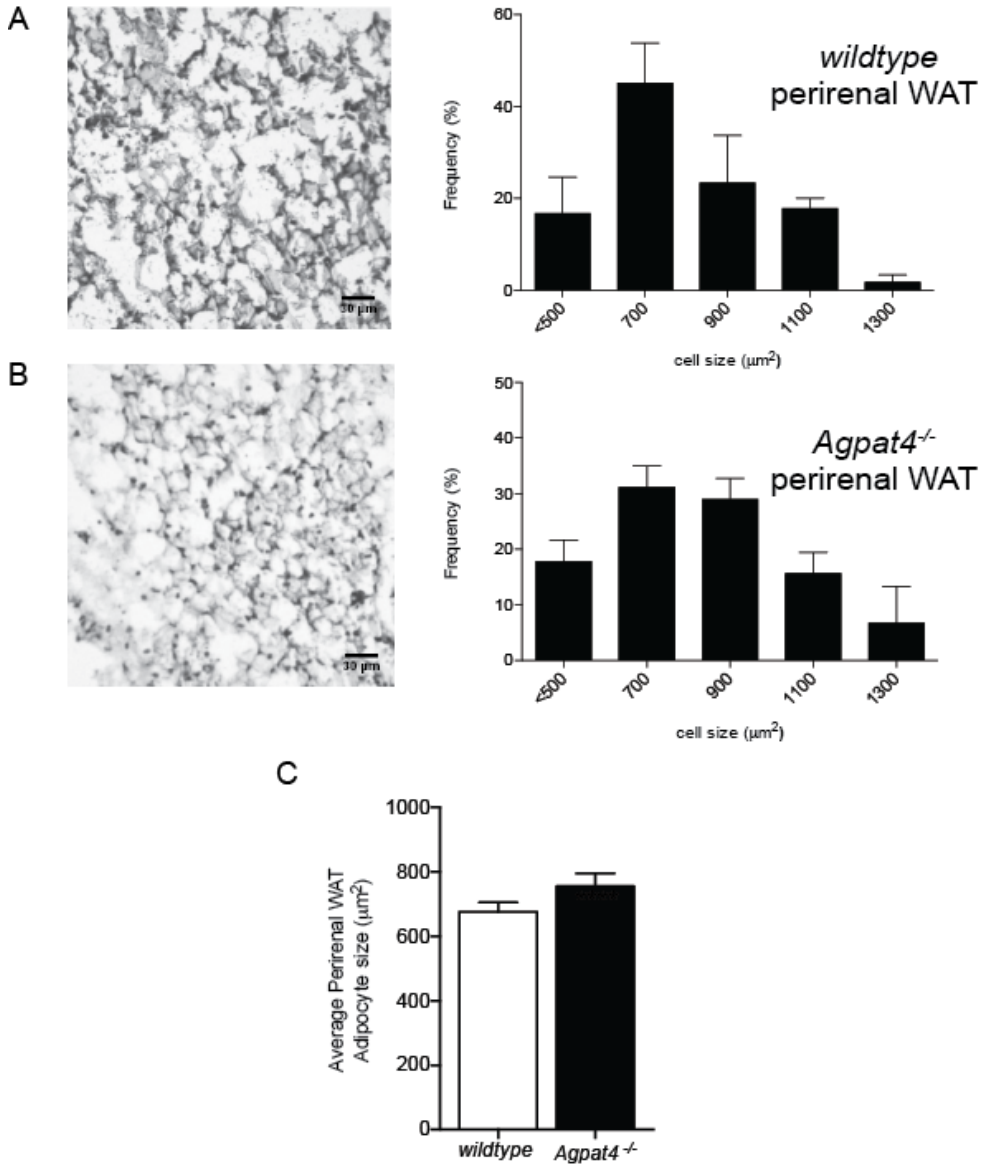

Figure 14. Adipocyte size in perirenal WAT. *A,* Representative image of *wildtype* hematoxylin & eosin-stained sections of perirenal WAT and frequency distribution of adipocyte cell size. *B,* Representative image of *Agpat4*$^{-/-}$ hematoxylin & eosin-stained sections of perirenal WAT and frequency distribution of adipocyte cell size. *C,* Average adipocyte cell size. (n=4). Data are means ± SEM.

Genes involved in TAG synthesis are upregulated in epididymal WAT of Agpat4$^{-/-}$ mice

To assess if the increase in TAG content and adipocyte size in the epididymal WAT of *Agpat4*$^{-/-}$ mice is due to an increase in TAG synthesis, expression of a panel of genes encoding Kennedy pathway enzymes was assessed by qPCR on epididymal WAT cDNA from *Agpat4*$^{-/-}$ and *wildtype* mice (Fig. 15A). Gene analysis using perirenal WAT was also performed (Fig. 15B). Results shown are expressed relative to 18S. In epididymal WAT from *Agpat4*$^{-/-}$ mice, expression of two lipid synthetic genes was elevated. Expression of the gene encoding LIPIN1 was significantly higher (2.3-fold) as well as expression of the gene encoding DGAT1 (2.0-fold). There were no significant differences in the expression of *Dgat2*, *Cds1*, *Cds2*, *Cdipt*, *Pgs1*, *Cept1*, or *Chpt1*. No significant differences were seen for perirenal WAT in the expression of any of the genes encoding Kennedy pathway proteins.

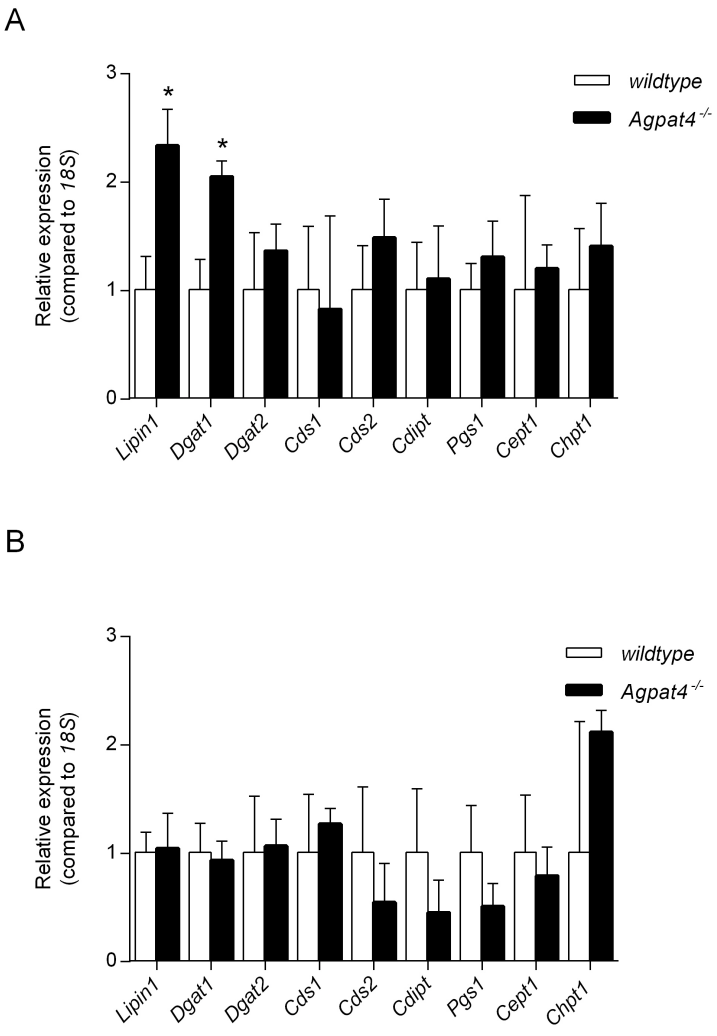

Figure 15. Kennedy pathway gene expression analysis. Analysis of expression of genes encoding enzymes involved in the Kennedy pathway in *Agpat4*$^{-/-}$ *and wildtype* mice from *A,* epididymal WAT and *B,* perirenal WAT. (n=5-7). Data are ± SEM. *P < 0.05 vs. *wildtype*.

Fatty acid synthesis enzymes are not altered in Agpat4$^{-/-}$ mice in epididymal or perirenal WAT

To assess if the increase in TAG content or fatty acid composition is due to an increase in fatty acid metabolism in the *Agpat4*$^{-/-}$ mice, immunoblotting was utilized to measure the protein content of various enzymes involved in fatty acid metabolism in epididymal white adipose tissue (Fig. 16) and perirenal white adipose tissue (Fig. 17). The results are expressed relative to total protein content per lane. There were no significant differences found in the protein content of ACC, P-ACC S79, AMPK α, or FAS between *Agpat4*$^{-/-}$ and *wildtype* mice in either the epididymal or perirenal adipose depots.

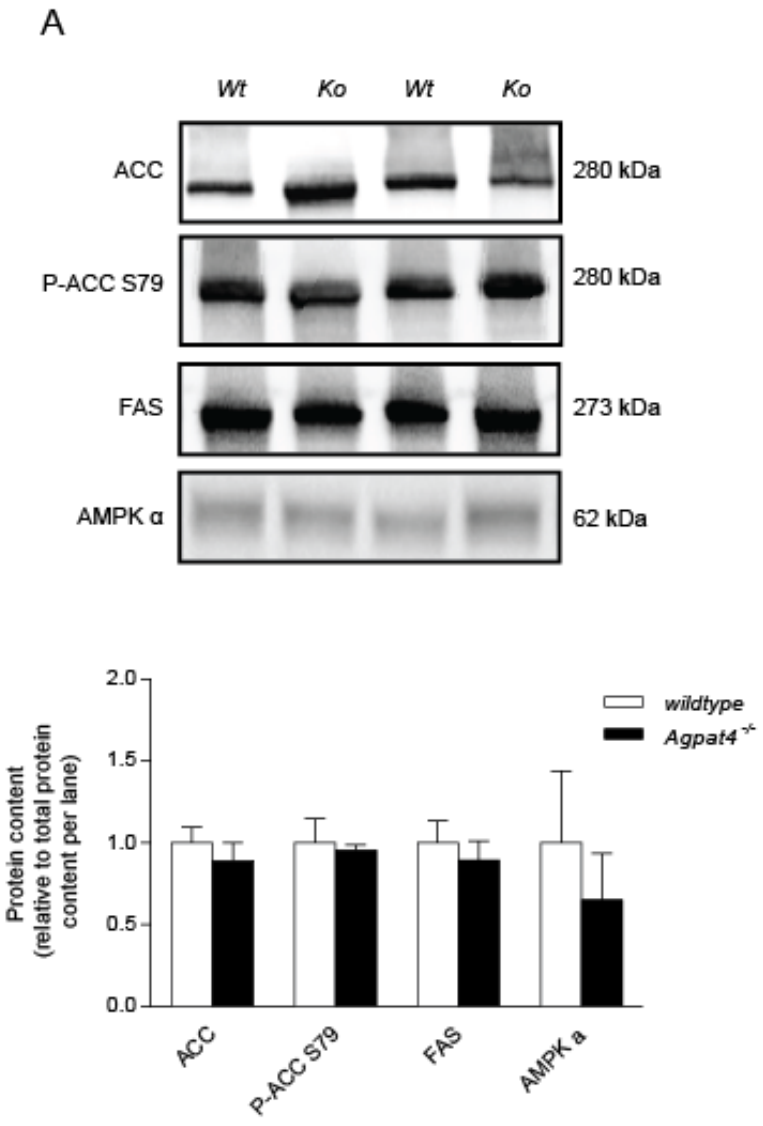

Figure 16. Levels of epididymal WAT enzymes involved in *de novo* fatty acid synthesis. Shown are *A*, Western blots and *B,* relative quantification, for ACC, P-ACC S79, AMPK α, and FAS from epididymal WAT in *Agpat4*$^{-/-}$ and *wildtype* mice. (n=7-9). Data are ± SEM.

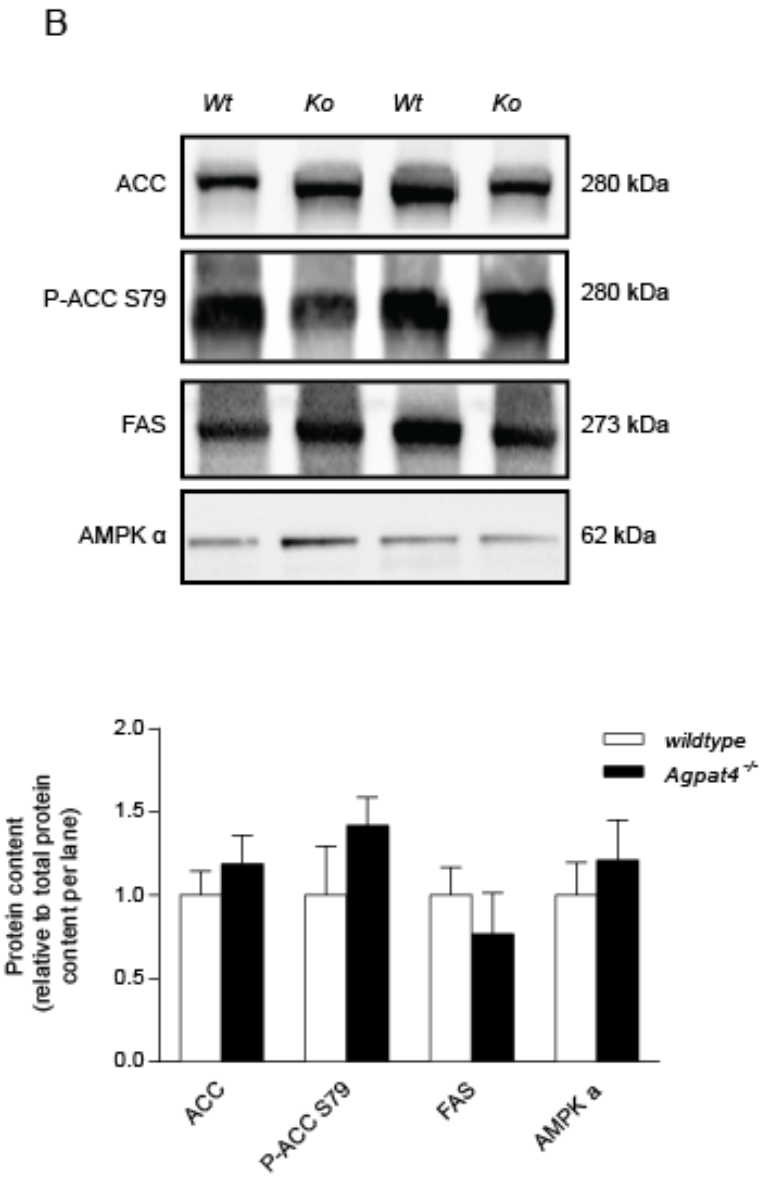

Figure 17. Levels of perirenal WAT enzymes involved in *de novo* fatty acid synthesis. Shown are *A*, Western blots and *B,* relative quantification, for ACC, P-ACC S79, AMPK α, and FAS from perirenal WAT in *Agpat4*$^{-/-}$ and *wildtype* mice. (n=7-9). Data are ± SEM.

Levels of enzymes involved in lipolysis are decreased in Agpat4$^{-/-}$ *mice in epididymal WAT*

In order to examine if the increase in TAG content in the epididymal adipose tissue of *Agpat4*$^{-/-}$ mice is due to a decrease in lipolysis, immunoblotting was utilized to assess levels of a panel of enzymes involved in the lipolysis pathway in *Agpat4*$^{-/-}$ and *wildtype* mice (Fig. 18). Perirenal adipose tissue was also analyzed (Fig. 19). In epididymal adipose tissue from *Agpat4*$^{-/-}$ mice, there was a significant ~50% decrease in ATGL content, a significant ~40% decrease in P-HSL S563 content, and a

significant ~60% decrease in P-HSL S660 content. No significant differences were observed in the content of HSL, P-HSL S565, or perilipin. The perirenal adipose tissue from *Agpat4*$^{-/-}$ mice showed no significant differences in the content of ATGL, HSL, P-HSL S563, P-HSL S565, P-HSL S660, or perilipin.

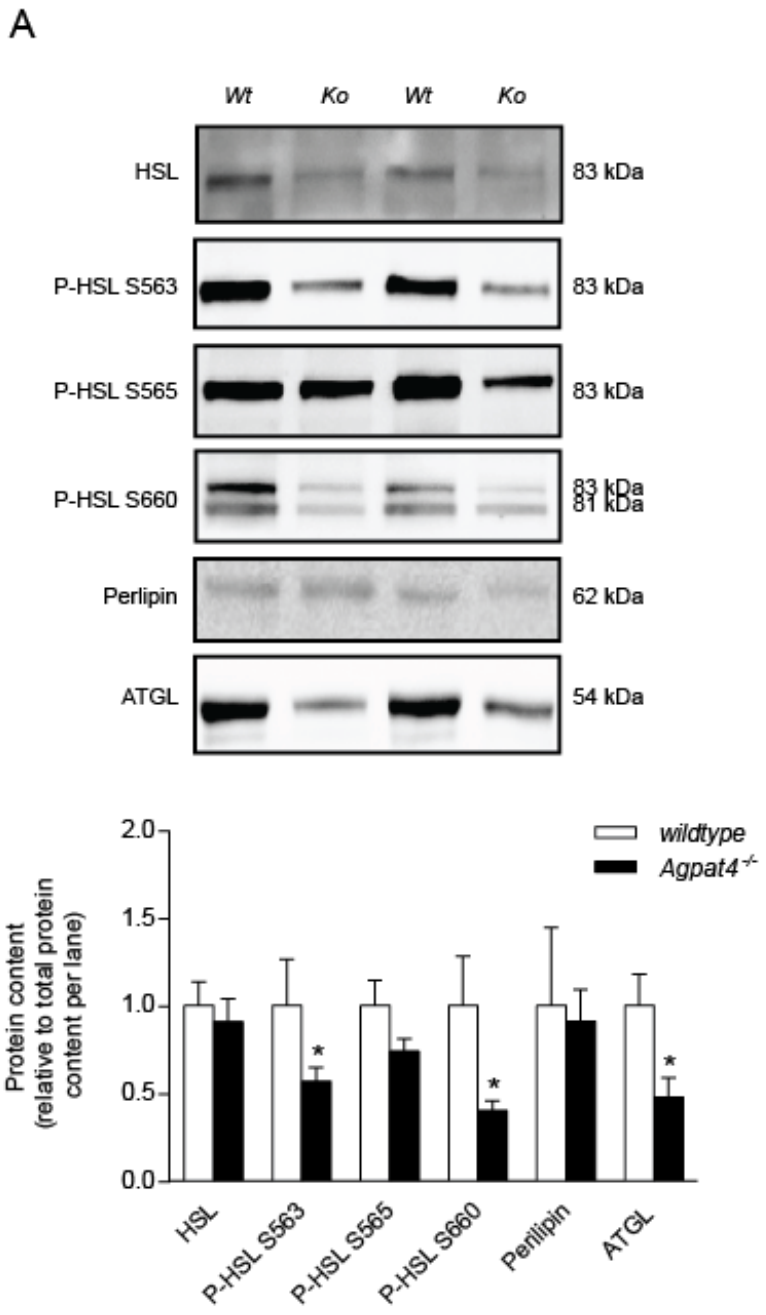

Figure 18. Levels of epididymal WAT enzymes involved in lipolysis. Shown are *A*, Western blots and *B,* relative quantification, for ATGL, HSL, P-HSL S563, P-HSL S565, P-HSL S660 and perilipin from epididymal WAT in *Agpat4*$^{-/-}$ and *wildtype* mice. (n=7-9). Data are ± SEM. *P < 0.05 vs. *wildtype*.

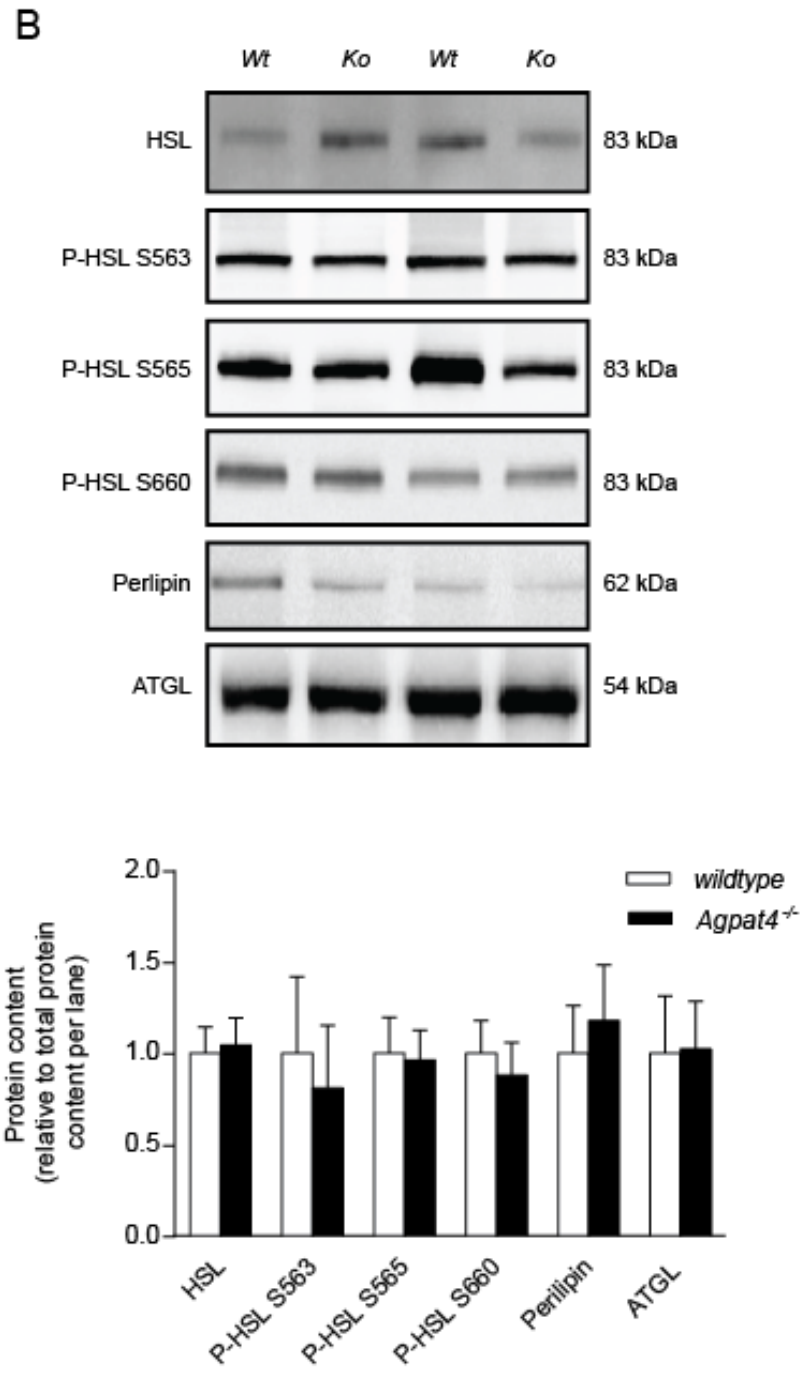

Figure 19. Levels of perirenal WAT enzymes involved in lipolysis. Shown are *A*, Western blots and *B,* relative quantification, for ATGL. HSL. P-HSL S563, P-HSL S565, P-HSL S660 and perilipin from perirenal WAT in *Agpat4*$^{-/-}$ and *wildtype* mice. (n=7-9). Data are ± SEM.

Lipolysis is decreased in Agpat4$^{-/-}$ mice in epididymal WAT

To determine if the decrease in protein content of enzymes involved in lipolysis corresponds to a decrease in lipolytic activity in the epididymal adipose depot of the *Agpat4*$^{-/-}$mice, an *in vitro* radiochemical triolein hydrolase assay was utilized. The amount of total triolein lipase activity, as measured by the production of ^{3}H-oleate, in *Agpat4*$^{-/-}$ and *wildtype* mice, was determined in extracts from epididymal adipose tissue (Fig. 20A) and compared to the perirenal adipose depot (Fig. 20B). The results are expressed as nmol [^{3}H]oleic acid hydrolyzed/min/mg protein. A significant ~30% decrease in ^{3}H-oleate was observed between the epididymal adipose tissue from *Agpat4*$^{-/-}$ mice and *wildtype* littermates (0.055 ± 0.0047 versus 0.039 ± 0.0055 nmol/min/mg protein) whereas no significant differences were seen for the perirenal adipose depot.

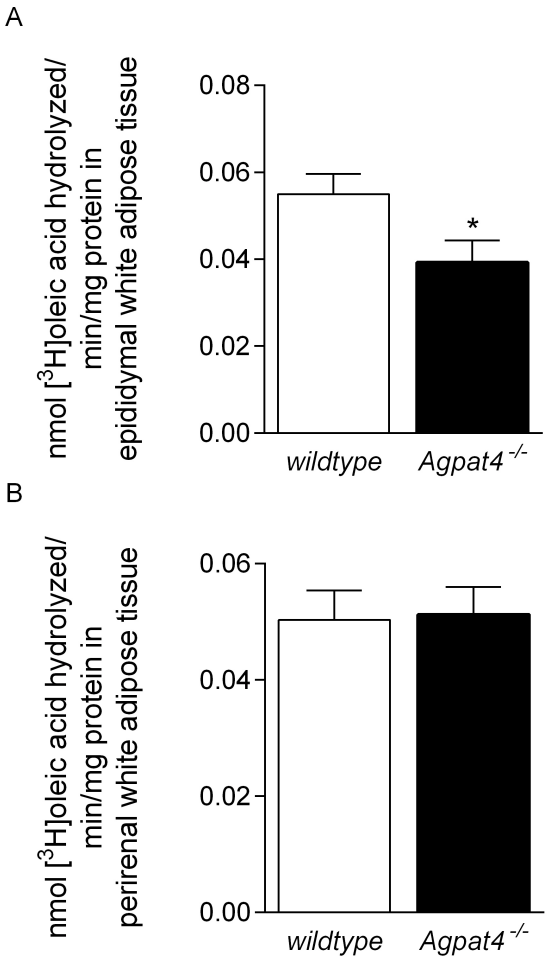

Figure 20. Triacylglycerol lipase activity in *Agpat4*$^{-/-}$ and *wildtype* mice. The amount of total triolein lipase activity, as measured by the production of ^{3}H-FA, in *Agpat4*$^{-/-}$ and *wildtype* mice. *A,* epididymal WAT. *B,* perirenal WAT. (n=6-7). Data are ± SEM. *P < 0.05 vs. *wildtype*.

To confirm the decrease in lipolysis in the epididymal WAT of *Agpat4*$^{-/-}$ mice, an *in situ* lipolysis assay was utilized in which glycerol and free fatty acid release was measured from epididymal tissue explants (Fig. 21). This was studied under both basal and dibutyryl-cAMP stimulated conditions. All findings are expressed as mg/ml, relative to basal release at time point 0 hours. In agreement with the findings from the *in vitro* triolein hydrolase assay, cAMP stimulated glycerol release was found to be significantly lower, by 16.9% at 2 hours (0.15 ± 0.043 versus 0.18 ± 0.0045 mg/ml glycerol released, $P<0.05$) and significantly lower by 13.5% at 4 hours (0.22 ± 0.0047 versus 0.25 ± 0.017 mg/ml glycerol released, $P<0.01$). Basal glycerol, basal NEFA, and cAMP-stimulated NEFA release from epididymal WAT explants, increased over time in both the *Agpat4*$^{-/-}$ and *wildtype* groups however, there were no statistically significant differences at any time point for these measures.

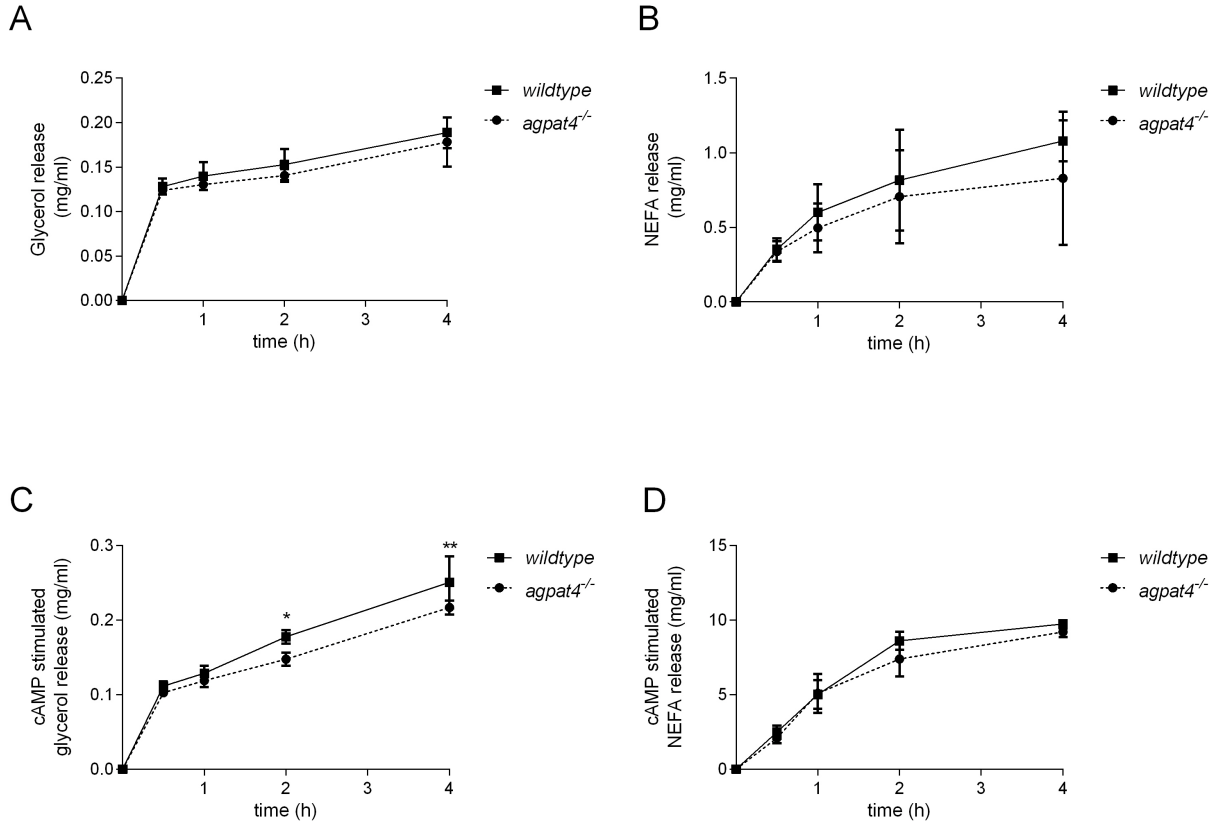

Figure 21. Glycerol and NEFA release from epididymal WAT explants. From the *in situ* lipolysis assay, using epididymal WAT tissue explants from *Agpat4*$^{-/-}$ and *wildtype* mice, the amount of *A,* glycerol release under unstimulated (basal) conditions. *B,* NEFA release under unstimulated (basal) conditions. *C,* glycerol release under dibutyryl-cAMP stimulated conditions. D, NEFA release under dibutyryl-cAMP stimulated conditions. (n=4). Data are ± SEM. *P < 0.05 vs. *wildtype*. **P < 0.01 vs. *wildtype*.

Plasma TAG and NEFA levels are unchanged in Agpat4$^{-/-}$ mice

To determine if the observed decrease in lipolysis in the epididymal WAT of *Agpat4*$^{-/-}$ mice is associated with changes in blood, plasma NEFA and TAG concentrations were determined (Fig. 22). Results are expressed in mg/dL. No statistically significant differences were found between *Agpat4*$^{-/-}$ mice and their *wildtype* littermates for plasma NEFA or plasma TAG.

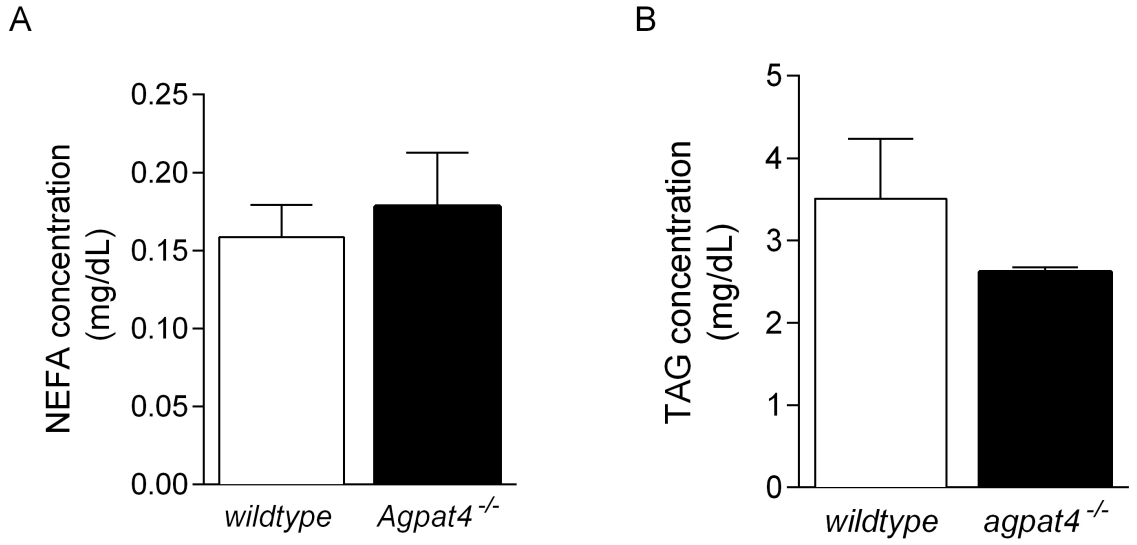

Figure 22. Plasma NEFA and TAG concentrations. Plasma concentration measurements in *Agpat4*$^{-/-}$ and *wildtype* mice for *A,* NEFA and *B,* TAG. (n=5). Data are ± SEM.

Other AGPAT isoforms are upregulated in perirenal WAT, but not epididymal WAT in Agpat4$^{-/-}$ mice

To investigate the observed differences between *Agpat4*$^{-/-}$ and *wildtype* mice in the epididymal WAT depot, relative to the lack of differences found in the perirenal WAT depot, RT-PCR was utilized to analyze the expression of the other AGPAT isoforms. Expression of *Agpat1, Agpat2, Agpat3,* and *Agpat5* was determined for both adipose tissue depots and results are expressed relative to *18S* expression (Fig. 23). No significant upregulation of *Agat1, Agpat2, Agpat3,* or *Agpat5* was found in the epididymal WAT of *Agpat4*$^{-/-}$ mice compared to their *wildtype* counterparts. In contrast, there was a significant 3.65-fold increase in the expression of *Agpat1*, a significant 3.36-fold increase in the expression of *Agpat2*, a significant 1.81-fold increase in the expression of *Agpat3*, and a significant 1.98-fold increase in the expression of *Agpat5* in the perirenal WAT of *Agpat4*$^{-/-}$ mice compared to their *wildtype* counterparts.

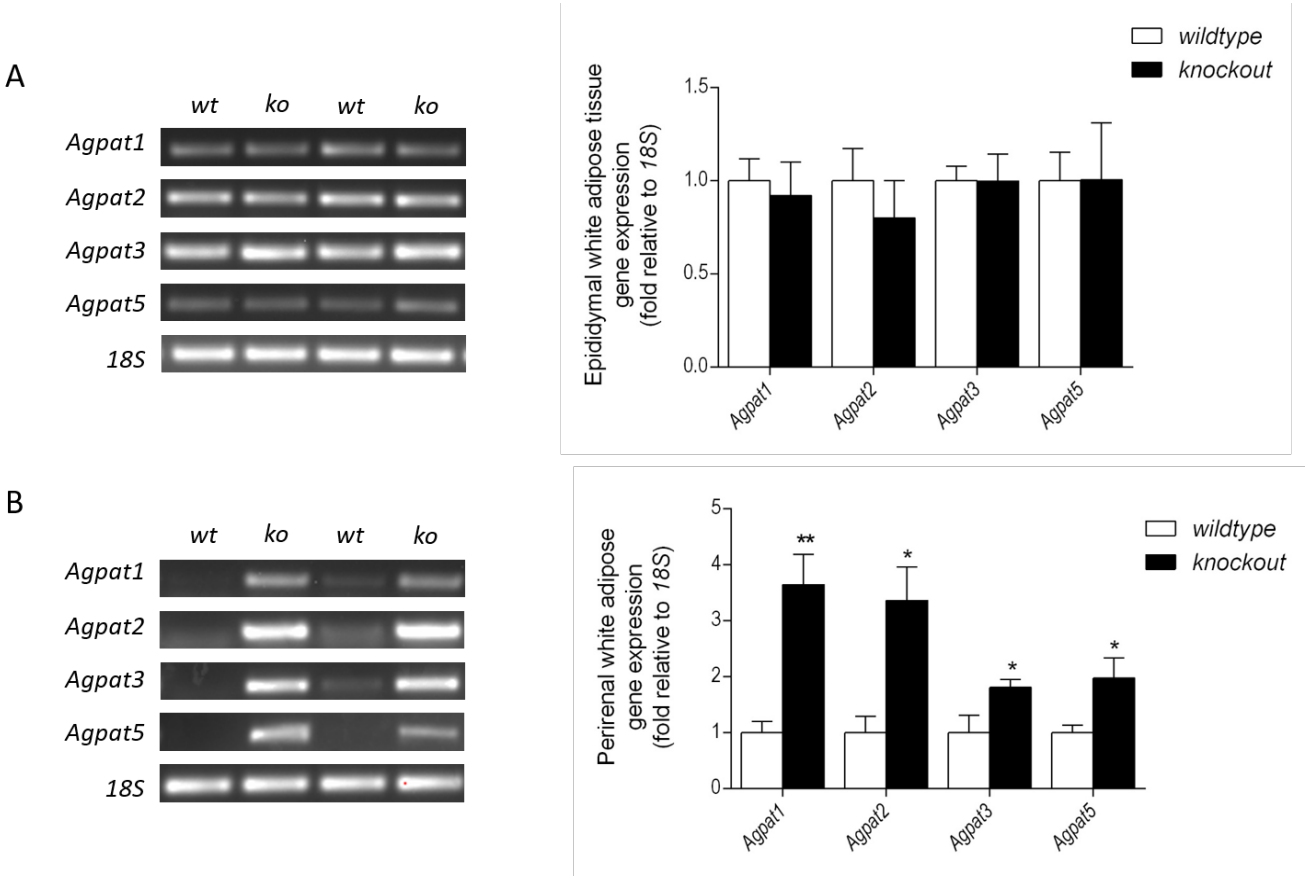

Figure 23. Expression of other AGPAT isoforms. Representative RT-PCR agarose image and quantification for *Agpat1, Agpat2, Agpat3,* and *Agpat5* in *A,* epididymal WAT and *B,* perirenal WAT. (n=4). Data are ± SEM. *P < 0.05 vs. control. **P < 0.01 vs. *wildtype*.

Chapter 6: Discussion

The AGPAT family of enzymes contains five true AGPAT isoforms, each showing different tissue expression patterns and functional preferences (18). We have shown previously that AGPAT4 is highly expressed in the brain (48, 64) and here we demonstrate that it is also abundant in various adipose depots including epididymal white adipose, perirenal white adipose, retroperitoneal white adipose, inguinal white adipose, and subscapular brown adipose tissue. (BAT). WAT is currently known to highly express AGPAT2 and AGPAT6, which both have been shown to play a significant role in determining TAG content. Therefore, we investigated the role of AGPAT4 in white adipose tissue using a gene ablation model.

Initially, we hypothesized that mice deficient for AGPAT4 would exhibit an impaired ability to produce TAG since the AGPAT family of enzymes function in the production of PA, the branching point for TAG and glycerophospholipid synthesis. We also hypothesized that this would result in decreased adipose tissue depot weights, as well as a decrease in whole body mass. Surprisingly, we found that loss of *Agpat4* did not result in a change in whole body weights or a significant change in the weights of the perirenal, retroperitoneal, inguinal, or subscapular brown adipose depots, but a significant increase in the weight of the epididymal white adipose depot. This is in contrast to *Agpat2*$^{-/-}$ mice, which demonstrate a complete absence of both WAT and BAT, although these mice did not have a difference in body weights since TAG was stored ectopically in organs throughout the body, most notably, the liver (78). This is also in contrast to *Agpat6*$^{-/-}$ mice, which have adipose tissue, but exhibit reduced TAG contents in WAT, reduced adipocyte size in epididymal WAT, and a decrease in total body weights stemming from increased energy expenditure, resulting in resistance to diet-induced obesity (67).

To explain the unanticipated phenotype of epididymal WAT in *Agpat4*$^{-/-}$ mice, we first investigated measures of whole body physiology, including food intake, activity, and energy metabolism, but failed to find any significant differences. This suggests that AGPAT4 does not play a critical role in determining RER, the ratio of carbon dioxide (VCO_2) to oxygen consumption (VO_2) which indicates which fuel source is being primarily metabolized. AGPAT4 was also shown to not play a critical role in determining the amount of heat expended, fat and carbohydrate oxidation, amount of food intake, total activity or dual beam and Z axis movement, as well as daily average VO_2, VO_2 awake, or VO_2 sleeping.

We next investigated the nature of the difference in epididymal WAT, and found that the larger depot size in *Agpat4*-deficient mice was associated with a greater content of total TAG, which

was predominantly acylated with saturated and monounsaturated fatty acids. In contrast, perirenal WAT depots, which did not differ in mass between *wildtype* and *Agpat4*$^{-/-}$ mice, exhibited no difference in TAG content or TAG fatty acyl composition. The observed increase in depot-specific TAG content may be attributed to a either a difference in adipocyte cell size, which is strongly suggested by the normalized increase in TAG content of epididymal WAT, or a difference in adipocyte differentiation (20, 77, 79).

Loss of *Agpat4* did not significantly alter the expression level of adipogenic marker genes including *C/ebpα, C/ebpβ, Pref-1, Pparγ, iPlaβ, iPlaγ, Ap2/Fabp4,* or *Fat/Cd36*, suggesting normal adipocyte differentiation in both the epididymal and perirenal WAT depots. This finding was somewhat unexpected, since we hypothesized that ablation of an AGPAT isoform would potentially result in a build-up of its substrate, LPA, which has been shown to have a key role in inhibition of adipogenesis (80). The lack of change in expression of key transcriptional activators of the adipogenic program in *Agpat4*$^{-/-}$ mice suggests that the role of AGPAT4 in determining TAG content is independent of alterations in adipocyte differentiation. In agreement, histological analysis revealed a greater frequency of larger adipocytes in the epididymal WAT of *Agpat4*$^{-/-}$ mice, and a statistically significant increase in average adipocyte size. This strongly suggests that larger epididymal depots in *Agpat4*$^{-/-}$ mice result from increases in adipocyte cell size rather than number. As expected, we did not observe a difference in adipocyte cell size frequency, or a change in average adipocyte size, in perirenal WAT.

Lipogenesis and lipolysis are major biochemical functions of adipose tissue that regulate TAG content. Determination of changes in these processes may provide mechanistic insight into the observed increase in TAG in the epididymal WAT of *Agpat4*$^{-/-}$ mice. Expression level was measured for genes encoding Kennedy pathway proteins as well as the protein content of enzymes involved in fatty acid synthesis. No differences were found in epididymal WAT for the expression of *Cds1, Cds2, Cdipt, Pgs1, Cept1,* or *Chpt1*, which code for proteins involved in the formation of PI, PE, PC, PG, PS, and CL or for the content of ACC, P-ACC S79, AMPK α or FAS, which participate in the *de novo* synthesis of fatty acids. However, an upregulation was observed in the expression of *Lipin1*, the gene encoding the enzyme PAP, which catalyzes the formation of DAG from PA in a step that is critical for TAG synthesis (34). In addition, *Dgat1* was upregulated, although *Dgat2* was not. Both isoforms are highly expressed in WAT and are involved in the formation of TAG from DAG, but do not show sequence or protein homology, and have been shown to have distinct physiological roles through the generation of gene ablation models (36, 81-83). A mouse overexpression model of DGAT1, but not DGAT2, has been shown to increase liver VLDL secretion, resulting in increased

epididymal WAT weight (84). This was attributed to the high expression of the VLDL receptor in the epididymal fat pad causing a VLDL-mediated increase in epididymal WAT mass (84). These findings suggest that the increased *Dgat1* expression in the epididymal WAT depot in *Agpat4*$^{-/-}$ mice may be contributing to the increase in total cellular TAG content either directly, through the conversion of DAG to TAG, or indirectly, through an increase in the uptake of VLDL. Together, these results indicate that *Agpat4* ablation has little effect on phospholipid synthesizing enzymes or on early steps in TAG synthesis including *de novo* lipogenesis, but does appear to promote enzymatic steps in formation of TAG, specifically. No differences were found in the perirenal WAT depot with regards to the expression of any Kennedy pathway marker genes or enzymes involved in fatty acid synthesis.

We also explored whether changes in TAG lipolysis could help explain the increase in epididymal WAT weight, adipocyte size, and TAG content. A decrease in HSL phosphorylated at the serine 563 and 660 sites, as well as total ATGL, was observed in the epididymal WAT of *Agpat4*$^{-/-}$, while no differences were observed in the amounts of total HSL, HSL phosphorylated at the S565 site, or perilipin. The increase in protein content of lipolytic enzymes was accompanied by a 30% increase in total triolein hydrolase activity. No differences were observed in lipolytic proteins or triolein lipase activity in perirenal WAT. Adipocyte lipolysis is activated during times of energy deprivation. This increases hydrolytic activity of ATGL, which cleaves a fatty acyl chain from the *sn*-2 position of TAG forming DAG, and HSL, which subsequently cleaves a fatty acyl chain from the *sn*-1 or *sn*-3 positions of DAG to produce MAG (20). During lipolysis stimulation, intracellular cAMP levels increase, activating cAMP-dependent PKA to phosphorylate HSL at the serine residues 563 and 660, causing translocation of the enzyme to the lipid droplet (21). These findings therefore, suggest a decrease in cAMP-stimulated lipolytic activity in the epididymal WAT of Agpat4$^{-/-}$ mice. *In situ* analysis supported this contention, since there were no significant differences between *wildtype* and *Agpat4*$^{-/-}$ littermates when glycerol and NEFA release were assessed under basal conditions, but there was a significant reduction in glycerol release from epididymal WAT explants stimulated with dibutyryl cAMP. Interestingly, there were no corresponding significant differences in NEFA release from epididymal WAT explants under stimulated conditions. Glycerol is produced when lipolysis proceeds to completion, and is exported from adipocytes that lack glycerol kinase activity and therefore cannot reutilize this structure in lipid synthesis. NEFA, however, can be used directly in adipocytes, either for re-esterification into complex lipids, or for beta-oxidation and energy provision. No significant differences were found in plasma TAG and NEFA levels, further suggesting increased re-esterification of released NEFA in adipose tissue of *Agpat4*$^{-/-}$ epididymal

WAT. Further study however, will be required to determine the major metabolic fate(s) of lipolysis-derived fatty acids from *Agpat4*$^{-/-}$ epididymal WAT.

In perirenal WAT, PA levels were not significantly different between *wildtype* and *Agpat4*$^{-/-}$ mice. As was observed previously in brain, a compensatory upregulation of other AGPAT isoforms may aid in explaining this (48). In perirenal WAT, loss of *Agpat4* resulted in increased gene expression of the other true AGPAT/LPAAT isoforms, *Agpat1*, *Agpat2*, *Agpat3*, and *Agpat5*. Importantly, this appears to have both normalized PA content, and preserved biochemical and physiological functioning of this WAT depot, since no differences in TAG or other PL species were observed, and no differences in lipolysis, lipogenesis, or apparent differentiation were detected. This finding is in contrast to our previous observations in brain, where loss of Agpat4 did not reduce total PA level, but did reduce levels of PC, PE, and PI (48).

In contrast, PA levels were significantly elevated in epididymal WAT from *Agpat4*$^{-/-}$ mice compared to *wildtype* littermates, and yet we observed no difference in expression of the other *Agpat* isoforms in this depot. It has been shown that AGPAT isoforms 1, 3, and 5 are significantly upregulated in the livers of male *Agpat2*$^{-/-}$ mice (78), but are downregulated in *Agpat2* knockdown OP9 cells (69). Taken together with findings from the current study, this indicates that the coordinated response of different AGPAT isoforms is not only tissue-specific, but also depot-specific with regards to adipose tissue. This finding has particular importance for adipose tissue biology research, since it indicates a startling heterogeneity in the molecular physiology of closely positioned depots that are often considered as a single entity (i.e. “visceral adipose tissue”).

When considered relative to findings in perirenal WAT, it seems highly likely that the absence of a compensatory upregulation of the other AGPAT isoforms, and the paradoxical elevation in epididymal WAT PA levels, are causal in generating the marked changes observed specifically in this depot. PA is a precursor for TAG synthesis, and while the source of increased epididymal PA content remains undetermined, upregulated *Lipin1* and *Dgat1* expression suggest it is likely utilized to increase TAG production. PA is also involved in the biophysical processes underlying lipid droplet formation and lipid droplet TAG accretion, and therefore may directly promote the enhanced storage of lipid in this tissue (85, 86). For example, in brown adipose tissue, lipid droplets have been shown to enlarge through the docking of two lipid droplets and subsequently, the transference of lipids between the pairs. This process is facilitated by the amphipathic helix of CIDEA, a protein that interacts with PA on the lipid droplet phospholipid monolayer to increase phospholipid barrier permeability (85). In addition, PA is an allosteric activator of phosphodiesterase 4, which hydrolyzes cAMP to decrease activation of PKA (87, 88). It is therefore, highly plausible that decreased

stimulated lipolysis in epididymal WAT from *Agpat4*$^{-/-}$ mice resulted, at least in part, from elevated tissue levels of PA. With regards to differentiation, PA has been found to block the differentiation of cultured 3T3-L1 adipocytes, but overexpression of *Lipin1* can rescue this (89). In epididymal WAT from Agpat4$^{-/-}$ mice, elevated PA content was observed together with an upregulation of *Lipin1*, and therefore these two effects may have prevented any adverse effects on adipocyte differentiation.

In summary, we have characterized two closely positioned visceral WAT depots from *Agpat4*$^{-/-}$ mice and their *wildtype* littermates. Although perirenal and epididymal WAT express similar levels of *Agpat4*, we have found differences between these two depots in the biochemistry, molecular physiology, functional processes, and compensatory responses, as a result of loss of this isoform. In perirenal WAT, an induction of the other *Agpat/Lpaat* isoforms (1, 2, 3, and 5) resulted in an essentially perfect compensation with regards to restoration of cellular PA levels, as well as maintenance of all cellular processes in a state that was indistinguishable from *wildtype*. In epididymal WAT however, there was no compensatory induction of the other *Agpat/Lpaats*, and metabolic perturbations were evident in most biochemical and physiological processes examined. This work therefore provides novel information on the differential role of *Agpat4* in perirenal and epididymal WAT, highlighting important differences between these two depots.

Chapter 7: Study limitations and future directions

Limitations

The foremost limitation in this study of characterizing the critical role of AGPAT4 in white adipose tissue is the use of a global *Agpat4*$^{-/-}$ mouse model. Although the model aids in examining the effect of total loss of AGPAT4, it fails to elucidate the white adipose tissue specific effects that it plays. The findings in this study may, in part, be explained by other changes in the global *Agpat4*$^{-/-}$ model that are contributing to the differences within the epididymal WAT depot. Immortalized depot-specific adipocyte cell lines would aid in elucidating the intrinsic biochemical differences between different visceral adipose depots as well as the role AGPAT4 plays in determining their physiology. Future work will aim to address these limitations.

Future Directions

Future studies will investigate the biological significance and consequences of our findings that increased TAG content and decreased lipolysis accompanies loss of *Agpat4* in the epididymal WAT depot. Of particular interest are the downstream effects on spermatogenesis and reproduction, since epididymal WAT is necessary for these processes (90). In male Syrian hamsters, the complete absence of epididymal WAT eliminated spermatogenesis, decreased seminiferous tubule size, and resulted in aspermatic ejaculate, with no changes in testosterone levels or behaviour (90). In the present study using *Agpat4* ablated mice, weights of testicular tissue were not altered, and reproduction was not prevented, although male to female sex ratios were altered (data not shown). Further examination of the differences between individual visceral WAT depots is also of interest. There are known disparities between visceral and subcutaneous WAT, such as developmental origin, metabolic activity, mitochondrial content, rate of lipolysis, and correlation to insulin resistance and other metabolic diseases (4, 11, 12, 91, 92). However, the present study suggests significant metabolic differences between individual visceral WAT depots. Further work will be needed to address the role of *Agpat4* in the formation of TAG in these depots, as well as the role of other *Agpats* in regulation of depot-specific characteristics.

Our studies with *Agpat4*-deficient mice demonstrate that AGPAT4 plays a non-redundant role in different visceral WAT depots, as well as in brain (48). The present study revealed new insight into the function of AGPAT4 in TAG accumulation and synthesis, as well as lipolysis, and underscores the complexity of the roles of the different AGPAT isoforms, as well as the complex regulation of different visceral WAT depots. Future studies will aim to delineate the mechanisms by which AGPAT4 mediates effects observed in epididymal WAT.

References

1. Lafontan, M. 2014. Adipose tissue and adipocyte dysregulation. *Diabetes & metabolism* **40**: 16-28.
2. Cinti, S. 2005. The adipose organ. *Prostaglandins, leukotrienes, and essential fatty acids* **73**: 9-15.
3. Trayhurn, P. 2005. Endocrine and signalling role of adipose tissue: new perspectives on fat. *Acta physiologica Scandinavica* **184**: 285-293.
4. Chau, Y. Y., R. Bandiera, A. Serrels, O. M. Martinez-Estrada, W. Qing, M. Lee, J. Slight, A. Thornburn, R. Berry, S. McHaffie, R. H. Stimson, B. R. Walker, R. M. Chapuli, A. Schedl, and N. Hastie. 2014. Visceral and subcutaneous fat have different origins and evidence supports a mesothelial source. *Nature cell biology* **16**: 367-375.
5. Ahmadian, M., R. E. Duncan, K. Jaworski, E. Sarkadi-Nagy, and H. S. Sul. 2007. Triacylglycerol metabolism in adipose tissue. *Future lipidology* **2**: 229-237.
6. Walley, A. J., A. I. Blakemore, and P. Froguel. 2006. Genetics of obesity and the prediction of risk for health. *Human molecular genetics* **15 Spec No 2**: R124-130.
7. Jo, J., O. Gavrilova, S. Pack, W. Jou, S. Mullen, A. E. Sumner, S. W. Cushman, and V. Periwal. 2009. Hypertrophy and/or Hyperplasia: Dynamics of Adipose Tissue Growth. *PLoS computational biology* **5**: e1000324.
8. Rutkowski, J. M., J. H. Stern, and P. E. Scherer. 2015. The cell biology of fat expansion. *The Journal of cell biology* **208**: 501-512.
9. Halberg, N., T. Khan, M. E. Trujillo, I. Wernstedt-Asterholm, A. D. Attie, S. Sherwani, Z. V. Wang, S. Landskroner-Eiger, S. Dineen, U. J. Magalang, R. A. Brekken, and P. E. Scherer. 2009. Hypoxia-inducible factor 1alpha induces fibrosis and insulin resistance in white adipose tissue. *Molecular and cellular biology* **29**: 4467-4483.
10. Bjorndal, B., L. Burri, V. Staalesen, J. Skorve, and R. K. Berge. 2011. Different adipose depots: their role in the development of metabolic syndrome and mitochondrial response to hypolipidemic agents. *Journal of obesity* **2011**: 490650.
11. Kraunsoe, R., R. Boushel, C. N. Hansen, P. Schjerling, K. Qvortrup, M. Stockel, K. J. Mikines, and F. Dela. 2010. Mitochondrial respiration in subcutaneous and visceral adipose tissue from patients with morbid obesity. *The Journal of physiology* **588**: 2023-2032.
12. Deveaud, C., B. Beauvoit, B. Salin, J. Schaeffer, and M. Rigoulet. 2004. Regional differences in oxidative capacity of rat white adipose tissue are linked to the mitochondrial content of mature adipocytes. *Molecular and cellular biochemistry* **267**: 157-166.
13. Virtanen, K. A., P. Lonnroth, R. Parkkola, P. Peltoniemi, M. Asola, T. Viljanen, T. Tolvanen, J. Knuuti, T. Ronnemaa, R. Huupponen, and P. Nuutila. 2002. Glucose uptake and perfusion in subcutaneous and visceral adipose tissue during insulin stimulation in nonobese and obese humans. *The Journal of clinical endocrinology and metabolism* **87**: 3902-3910.
14. Kletzien, R. F., S. D. Clarke, and R. G. Ulrich. 1992. Enhancement of adipocyte differentiation by an insulin-sensitizing agent. *Molecular pharmacology* **41**: 393-398.
15. Okuno, A., H. Tamemoto, K. Tobe, K. Ueki, Y. Mori, K. Iwamoto, K. Umesono, Y. Akanuma, T. Fujiwara, H. Horikoshi, Y. Yazaki, and T. Kadowaki. 1998. Troglitazone increases the number of small adipocytes without the change of white adipose tissue mass in obese Zucker rats. *The Journal of clinical investigation* **101**: 1354-1361.
16. Garg, A. 2006. Adipose tissue dysfunction in obesity and lipodystrophy. *Clinical cornerstone* **8 Suppl 4**: S7-s13.

17. Ali, A. T., W. E. Hochfeld, R. Myburgh, and M. S. Pepper. 2013. Adipocyte and adipogenesis. *European journal of cell biology* **92**: 229-236.
18. Lu, B., Y. J. Jiang, Y. Zhou, F. Y. Xu, G. M. Hatch, and P. C. Choy. 2005. Cloning and characterization of murine 1-acyl-sn-glycerol 3-phosphate acyltransferases and their regulation by PPARalpha in murine heart. *The Biochemical journal* **385**: 469-477.
19. Eichmann, T. O., M. Kumari, J. T. Haas, R. V. Farese, Jr., R. Zimmermann, A. Lass, and R. Zechner. 2012. Studies on the substrate and stereo/regioselectivity of adipose triglyceride lipase, hormone-sensitive lipase, and diacylglycerol-O-acyltransferases. *The Journal of biological chemistry* **287**: 41446-41457.
20. Duncan, R. E., M. Ahmadian, K. Jaworski, E. Sarkadi-Nagy, and H. S. Sul. 2007. Regulation of lipolysis in adipocytes. *Annual review of nutrition* **27**: 79-101.
21. Jaworski, K., E. Sarkadi-Nagy, R. E. Duncan, M. Ahmadian, and H. S. Sul. 2007. Regulation of triglyceride metabolism. IV. Hormonal regulation of lipolysis in adipose tissue. *American journal of physiology. Gastrointestinal and liver physiology* **293**: G1-4.
22. Kim, S. J., T. Tang, M. Abbott, J. A. Viscarra, Y. Wang, and H. S. Sul. 2016. AMPK Phosphorylates Desnutrin/ATGL and Hormone-Sensitive Lipase To Regulate Lipolysis and Fatty Acid Oxidation within Adipose Tissue. *Molecular and cellular biology* **36**: 1961-1976.
23. Sztalryd, C., G. Xu, H. Dorward, J. T. Tansey, J. A. Contreras, A. R. Kimmel, and C. Londos. 2003. Perilipin A is essential for the translocation of hormone-sensitive lipase during lipolytic activation. *The Journal of cell biology* **161**: 1093-1103.
24. Miyoshi, H., S. C. Souza, H. H. Zhang, K. J. Strissel, M. A. Christoffolete, J. Kovsan, A. Rudich, F. B. Kraemer, A. C. Bianco, M. S. Obin, and A. S. Greenberg. 2006. Perilipin promotes hormone-sensitive lipase-mediated adipocyte lipolysis via phosphorylation-dependent and -independent mechanisms. *The Journal of biological chemistry* **281**: 15837-15844.
25. Ahmadian, M., M. J. Abbott, T. Tang, C. S. Hudak, Y. Kim, M. Bruss, M. K. Hellerstein, H. Y. Lee, V. T. Samuel, G. I. Shulman, Y. Wang, R. E. Duncan, C. Kang, and H. S. Sul. 2011. Desnutrin/ATGL is regulated by AMPK and is required for a brown adipose phenotype. *Cell metabolism* **13**: 739-748.
26. Rosen, E. D., C. J. Walkey, P. Puigserver, and B. M. Spiegelman. 2000. Transcriptional regulation of adipogenesis. *Genes & development* **14**: 1293-1307.
27. Kennedy, E. P., and S. B. Weiss. 1956. The function of cytidine coenzymes in the biosynthesis of phospholipides. *The Journal of biological chemistry* **222**: 193-214.
28. Lands, W. E. 1958. Metabolism of glycerolipides; a comparison of lecithin and triglyceride synthesis. *The Journal of biological chemistry* **231**: 883-888.
29. Bell, R. M., and R. A. Coleman. 1980. Enzymes of glycerolipid synthesis in eukaryotes. *Annual review of biochemistry* **49**: 459-487.
30. Kume, K., and T. Shimizu. 1997. cDNA cloning and expression of murine 1-acyl-sn-glycerol-3-phosphate acyltransferase. *Biochemical and biophysical research communications* **237**: 663-666.
31. Carman, G. M., and G. S. Han. 2009. Phosphatidic acid phosphatase, a key enzyme in the regulation of lipid synthesis. *The Journal of biological chemistry* **284**: 2593-2597.
32. Paulus, H., and E. P. Kennedy. 1960. The enzymatic synthesis of inositol monophosphatide. *The Journal of biological chemistry* **235**: 1303-1311.
33. Li, G., S. Chen, M. N. Thompson, and M. L. Greenberg. 2007. New insights into the regulation of cardiolipin biosynthesis in yeast: implications for Barth syndrome. *Biochimica et biophysica acta* **1771**: 432-441.

34. Smith, S. W., S. B. Weiss, and E. P. Kennedy. 1957. The enzymatic dephosphorylation of phosphatidic acids. *The Journal of biological chemistry* **228**: 915-922.
35. Kuge, O., and M. Nishijima. 1997. Phosphatidylserine synthase I and II of mammalian cells. *Biochimica et biophysica acta* **1348**: 151-156.
36. Cases, S., S. J. Smith, Y. W. Zheng, H. M. Myers, S. R. Lear, E. Sande, S. Novak, C. Collins, C. B. Welch, A. J. Lusis, S. K. Erickson, and R. V. Farese, Jr. 1998. Identification of a gene encoding an acyl CoA:diacylglycerol acyltransferase, a key enzyme in triacylglycerol synthesis. *Proceedings of the National Academy of Sciences of the United States of America* **95**: 13018-13023.
37. Coleman, R. A., and D. P. Lee. 2004. Enzymes of triacylglycerol synthesis and their regulation. *Progress in lipid research* **43**: 134-176.
38. Yamashita, A., Y. Hayashi, Y. Nemoto-Sasaki, M. Ito, S. Oka, T. Tanikawa, K. Waku, and T. Sugiura. 2014. Acyltransferases and transacylases that determine the fatty acid composition of glycerolipids and the metabolism of bioactive lipid mediators in mammalian cells and model organisms. *Progress in lipid research* **53**: 18-81.
39. Yet, S. F., S. Lee, Y. T. Hahm, and H. S. Sul. 1993. Expression and identification of p90 as the murine mitochondrial glycerol-3-phosphate acyltransferase. *Biochemistry* **32**: 9486-9491.
40. Lewin, T. M., N. M. Schwerbrock, D. P. Lee, and R. A. Coleman. 2004. Identification of a new glycerol-3-phosphate acyltransferase isoenzyme, mtGPAT2, in mitochondria. *The Journal of biological chemistry* **279**: 13488-13495.
41. Cao, J., J. L. Li, D. Li, J. F. Tobin, and R. E. Gimeno. 2006. Molecular identification of microsomal acyl-CoA:glycerol-3-phosphate acyltransferase, a key enzyme in de novo triacylglycerol synthesis. *Proceedings of the National Academy of Sciences of the United States of America* **103**: 19695-19700.
42. Nagle, C. A., L. Vergnes, H. Dejong, S. Wang, T. M. Lewin, K. Reue, and R. A. Coleman. 2008. Identification of a novel sn-glycerol-3-phosphate acyltransferase isoform, GPAT4, as the enzyme deficient in Agpat6-/- mice. *Journal of lipid research* **49**: 823-831.
43. Bell, R. M., and R. A. Coleman. 1983. Enzymes of triacylglycerol formation in mammals *In* The Enzymes. P. D. Boyer, E. G. Krebs, and D. S. Sigman, editors. Academic Press New York. 87-112.
44. Sukumaran, S., R. I. Barnes, A. Garg, and A. K. Agarwal. 2009. Functional characterization of the human 1-acylglycerol-3-phosphate-O-acyltransferase isoform 10/glycerol-3-phosphate acyltransferase isoform 3. *Journal of molecular endocrinology* **42**: 469-478.
45. Chen, Y. Q., M. S. Kuo, S. Li, H. H. Bui, D. A. Peake, P. E. Sanders, S. J. Thibodeaux, S. Chu, Y. W. Qian, Y. Zhao, D. S. Bredt, D. E. Moller, R. J. Konrad, A. P. Beigneux, S. G. Young, and G. Cao. 2008. AGPAT6 is a novel microsomal glycerol-3-phosphate acyltransferase. *The Journal of biological chemistry* **283**: 10048-10057.
46. Agarwal, A. K., S. Sukumaran, V. A. Cortes, K. Tunison, D. Mizrachi, S. Sankella, R. D. Gerard, J. D. Horton, and A. Garg. 2011. Human 1-acylglycerol-3-phosphate O-acyltransferase isoforms 1 and 2: biochemical characterization and inability to rescue hepatic steatosis in Agpat2(-/-) gene lipodystrophic mice. *The Journal of biological chemistry* **286**: 37676-37691.
47. Yuki, K., H. Shindou, D. Hishikawa, and T. Shimizu. 2009. Characterization of mouse lysophosphatidic acid acyltransferase 3: an enzyme with dual functions in the testis. *Journal of lipid research* **50**: 860-869.
48. Bradley, R. M., P. M. Marvyn, J. J. Aristizabal Henao, E. B. Mardian, S. George, M. G. Aucoin, K. D. Stark, and R. E. Duncan. 2015. Acylglycerophosphate acyltransferase 4

(AGPAT4) is a mitochondrial lysophosphatidic acid acyltransferase that regulates brain phosphatidylcholine, phosphatidylethanolamine, and phosphatidylinositol levels. *Biochimica et biophysica acta* **1851**: 1566-1576.
49. Li, D., L. Yu, H. Wu, Y. Shan, J. Guo, Y. Dang, Y. Wei, and S. Zhao. 2003. Cloning and identification of the human LPAAT-zeta gene, a novel member of the lysophosphatidic acid acyltransferase family. *Journal of human genetics* **48**: 438-442.
50. Ye, G. M., C. Chen, S. Huang, D. D. Han, J. H. Guo, B. Wan, and L. Yu. 2005. Cloning and characterization a novel human 1-acyl-sn-glycerol-3-phosphate acyltransferase gene AGPAT7. *DNA sequence : the journal of DNA sequencing and mapping* **16**: 386-390.
51. Agarwal, A. K., R. I. Barnes, and A. Garg. 2006. Functional characterization of human 1-acylglycerol-3-phosphate acyltransferase isoform 8: cloning, tissue distribution, gene structure, and enzymatic activity. *Archives of biochemistry and biophysics* **449**: 64-76.
52. Agarwal, A. K., S. Sukumaran, R. Bartz, R. I. Barnes, and A. Garg. 2007. Functional characterization of human 1-acylglycerol-3-phosphate-O-acyltransferase isoform 9: cloning, tissue distribution, gene structure, and enzymatic activity. *The Journal of endocrinology* **193**: 445-457.
53. Agarwal, A. K., and A. Garg. 2010. Enzymatic activity of the human 1-acylglycerol-3-phosphate-O-acyltransferase isoform 11: upregulated in breast and cervical cancers. *Journal of lipid research* **51**: 2143-2152.
54. Lewin, T. M., P. Wang, and R. A. Coleman. 1999. Analysis of amino acid motifs diagnostic for the sn-glycerol-3-phosphate acyltransferase reaction. *Biochemistry* **38**: 5764-5771.
55. Cao, J., D. Shan, T. Revett, D. Li, L. Wu, W. Liu, J. F. Tobin, and R. E. Gimeno. 2008. Molecular identification of a novel mammalian brain isoform of acyl-CoA:lysophospholipid acyltransferase with prominent ethanolamine lysophospholipid acylating activity, LPEAT2. *The Journal of biological chemistry* **283**: 19049-19057.
56. Cao, J., Y. Liu, J. Lockwood, P. Burn, and Y. Shi. 2004. A novel cardiolipin-remodeling pathway revealed by a gene encoding an endoplasmic reticulum-associated acyl-CoA:lysocardiolipin acyltransferase (ALCAT1) in mouse. *The Journal of biological chemistry* **279**: 31727-31734.
57. Nakanishi, H., H. Shindou, D. Hishikawa, T. Harayama, R. Ogasawara, A. Suwabe, R. Taguchi, and T. Shimizu. 2006. Cloning and characterization of mouse lung-type acyl-CoA:lysophosphatidylcholine acyltransferase 1 (LPCAT1). Expression in alveolar type II cells and possible involvement in surfactant production. *The Journal of biological chemistry* **281**: 20140-20147.
58. Shindou, H., D. Hishikawa, H. Nakanishi, T. Harayama, S. Ishii, R. Taguchi, and T. Shimizu. 2007. A single enzyme catalyzes both platelet-activating factor production and membrane biogenesis of inflammatory cells. Cloning and characterization of acetyl-CoA:LYSO-PAF acetyltransferase. *The Journal of biological chemistry* **282**: 6532-6539.
59. Aguado, B., and R. D. Campbell. 1998. Characterization of a human lysophosphatidic acid acyltransferase that is encoded by a gene located in the class III region of the human major histocompatibility complex. *The Journal of biological chemistry* **273**: 4096-4105.
60. Hollenback, D., L. Bonham, L. Law, E. Rossnagle, L. Romero, H. Carew, C. K. Tompkins, D. W. Leung, J. W. Singer, and T. White. 2006. Substrate specificity of lysophosphatidic acid acyltransferase beta -- evidence from membrane and whole cell assays. *Journal of lipid research* **47**: 593-604.
61. Schmidt, J. A., and W. J. Brown. 2009. Lysophosphatidic acid acyltransferase 3 regulates Golgi complex structure and function. *The Journal of cell biology* **186**: 211-218.

62. Prasad, S. S., A. Garg, and A. K. Agarwal. 2011. Enzymatic activities of the human AGPAT isoform 3 and isoform 5: localization of AGPAT5 to mitochondria. *Journal of lipid research* **52**: 451-462.
63. Bradley, R. M. 2014

. Functional Characterization of murine 1-acylglycerol-3-phosphate O-acyltransferase 4 (AGPAT4) University of Waterloo, Waterloo, Ontario.
64. Bradley, R. M., E. B. Mardian, P. M. Marvyn, M. S. Vasefi, M. A. Beazely, J. G. Mielke, and R. E. Duncan. 2016. Data on acylglycerophosphate acyltransferase 4 (AGPAT4)during murine embryogenesis and in embryo-derived cultured primary neurons and glia. *Data in Brief* **6**: 28-32.
65. Li, J., C. Romestaing, X. Han, Y. Li, X. Hao, Y. Wu, C. Sun, X. Liu, L. S. Jefferson, J. Xiong, K. F. Lanoue, Z. Chang, C. J. Lynch, H. Wang, and Y. Shi. 2010. Cardiolipin remodeling by ALCAT1 links oxidative stress and mitochondrial dysfunction to obesity. *Cell metabolism* **12**: 154-165.
66. Cao, J., S. Perez, B. Goodwin, Q. Lin, H. Peng, A. Qadri, Y. Zhou, R. W. Clark, M. Perreault, J. F. Tobin, and R. E. Gimeno. 2014. Mice deleted for GPAT3 have reduced GPAT activity in white adipose tissue and altered energy and cholesterol homeostasis in diet-induced obesity. *American journal of physiology. Endocrinology and metabolism* **306**: E1176-1187.
67. Vergnes, L., A. P. Beigneux, R. Davis, S. M. Watkins, S. G. Young, and K. Reue. 2006. Agpat6 deficiency causes subdermal lipodystrophy and resistance to obesity. *Journal of lipid research* **47**: 745-754.
68. Agarwal, A. K., E. Arioglu, S. De Almeida, N. Akkoc, S. I. Taylor, A. M. Bowcock, R. I. Barnes, and A. Garg. 2002. AGPAT2 is mutated in congenital generalized lipodystrophy linked to chromosome 9q34. *Nature genetics* **31**: 21-23.
69. Gale, S. E., A. Frolov, X. Han, P. E. Bickel, L. Cao, A. Bowcock, J. E. Schaffer, and D. S. Ory. 2006. A regulatory role for 1-acylglycerol-3-phosphate-O-acyltransferase 2 in adipocyte differentiation. *The Journal of biological chemistry* **281**: 11082-11089.
70. Eto, M., H. Shindou, and T. Shimizu. 2014. A novel lysophosphatidic acid acyltransferase enzyme (LPAAT4) with a possible role for incorporating docosahexaenoic acid into brain glycerophospholipids. *Biochemical and biophysical research communications* **443**: 718-724.
71. Lexicon Genetics MRRC UC Davis. 2010. *In*.
72. Schneider, C. A., W. S. Rasband, and K. W. Eliceiri. 2012. NIH Image to ImageJ: 25 years of image analysis. *Nature methods* **9**: 671-675.
73. Folch, J., M. Lees, and G. H. Sloane Stanley. 1957. A simple method for the isolation and purification of total lipides from animal tissues. *The Journal of biological chemistry* **226**: 497-509.
74. Metherel, A. H., A. Y. Taha, H. Izadi, and K. D. Stark. 2009. The application of ultrasound energy to increase lipid extraction throughput of solid matrix samples (flaxseed). *Prostaglandins, leukotrienes, and essential fatty acids* **81**: 417-423.
75. Bligh, E. G., and W. J. Dyer. 1959. A rapid method of total lipid extraction and purification. *Canadian journal of biochemistry and physiology* **37**: 911-917.
76. Ahmadian, M., R. E. Duncan, K. A. Varady, D. Frasson, M. K. Hellerstein, A. L. Birkenfeld, V. T. Samuel, G. I. Shulman, Y. Wang, C. Kang, and H. S. Sul. 2009. Adipose overexpression of desnutrin promotes fatty acid use and attenuates diet-induced obesity. *Diabetes* **58**: 855-866.

77. Gregoire, F. M., C. M. Smas, and H. S. Sul. 1998. Understanding adipocyte differentiation. *Physiological reviews* **78**: 783-809.
78. Cortes, V. A., D. E. Curtis, S. Sukumaran, X. Shao, V. Parameswara, S. Rashid, A. R. Smith, J. Ren, V. Esser, R. E. Hammer, A. K. Agarwal, J. D. Horton, and A. Garg. 2009. Molecular mechanisms of hepatic steatosis and insulin resistance in the AGPAT2-deficient mouse model of congenital generalized lipodystrophy. *Cell metabolism* **9**: 165-176.
79. Spalding, K. L., E. Arner, P. O. Westermark, S. Bernard, B. A. Buchholz, O. Bergmann, L. Blomqvist, J. Hoffstedt, E. Naslund, T. Britton, H. Concha, M. Hassan, M. Ryden, J. Frisen, and P. Arner. 2008. Dynamics of fat cell turnover in humans. *Nature* **453**: 783-787.
80. Simon, M. F., D. Daviaud, J. P. Pradere, S. Gres, C. Guigne, M. Wabitsch, J. Chun, P. Valet, and J. S. Saulnier-Blache. 2005. Lysophosphatidic acid inhibits adipocyte differentiation via lysophosphatidic acid 1 receptor-dependent down-regulation of peroxisome proliferator-activated receptor gamma2. *The Journal of biological chemistry* **280**: 14656-14662.
81. Cases, S., S. J. Stone, P. Zhou, E. Yen, B. Tow, K. D. Lardizabal, T. Voelker, and R. V. Farese, Jr. 2001. Cloning of DGAT2, a second mammalian diacylglycerol acyltransferase, and related family members. *The Journal of biological chemistry* **276**: 38870-38876.
82. Smith, S. J., S. Cases, D. R. Jensen, H. C. Chen, E. Sande, B. Tow, D. A. Sanan, J. Raber, R. H. Eckel, and R. V. Farese, Jr. 2000. Obesity resistance and multiple mechanisms of triglyceride synthesis in mice lacking Dgat. *Nature genetics* **25**: 87-90.
83. Stone, S. J., H. M. Myers, S. M. Watkins, B. E. Brown, K. R. Feingold, P. M. Elias, and R. V. Farese, Jr. 2004. Lipopenia and skin barrier abnormalities in DGAT2-deficient mice. *The Journal of biological chemistry* **279**: 11767-11776.
84. Yamazaki, T., E. Sasaki, C. Kakinuma, T. Yano, S. Miura, and O. Ezaki. 2005. Increased very low density lipoprotein secretion and gonadal fat mass in mice overexpressing liver DGAT1. *The Journal of biological chemistry* **280**: 21506-21514.
85. Barneda, D., J. Planas-Iglesias, M. L. Gaspar, D. Mohammadyani, S. Prasannan, D. Dormann, G. S. Han, S. A. Jesch, G. M. Carman, V. Kagan, M. G. Parker, N. T. Ktistakis, J. Klein-Seetharaman, A. M. Dixon, S. A. Henry, and M. Christian. 2015. The brown adipocyte protein CIDEA promotes lipid droplet fusion via a phosphatidic acid-binding amphipathic helix. *eLife* **4**: e07485.
86. Fei, W., G. Shui, Y. Zhang, N. Krahmer, C. Ferguson, T. S. Kapterian, R. C. Lin, I. W. Dawes, A. J. Brown, P. Li, X. Huang, R. G. Parton, M. R. Wenk, T. C. Walther, and H. Yang. 2011. A role for phosphatidic acid in the formation of "supersized" lipid droplets. *PLoS genetics* **7**: e1002201.
87. Savany, A., C. Abriat, G. Nemoz, M. Lagarde, and A. F. Prigent. 1996. Activation of a cyclic nucleotide phosphodiesterase 4 (PDE4) from rat thymocytes by phosphatidic acid. *Cellular signalling* **8**: 511-516.
88. Mitra, M. S., Z. Chen, H. Ren, T. E. Harris, K. T. Chambers, A. M. Hall, K. Nadra, S. Klein, R. Chrast, X. Su, A. J. Morris, and B. N. Finck. 2013. Mice with an adipocyte-specific lipin 1 separation-of-function allele reveal unexpected roles for phosphatidic acid in metabolic regulation. *Proceedings of the National Academy of Sciences of the United States of America* **110**: 642-647.
89. Zhang, P., K. Takeuchi, L. S. Csaki, and K. Reue. 2012. Lipin-1 phosphatidic phosphatase activity modulates phosphatidate levels to promote peroxisome proliferator-activated receptor gamma (PPARgamma) gene expression during adipogenesis. *The Journal of biological chemistry* **287**: 3485-3494.

90. Chu, Y., G. G. Huddleston, A. N. Clancy, R. B. Harris, and T. J. Bartness. 2010. Epididymal fat is necessary for spermatogenesis, but not testosterone production or copulatory behavior. *Endocrinology* **151**: 5669-5679.
91. Wajchenberg, B. L. 2000. Subcutaneous and visceral adipose tissue: their relation to the metabolic syndrome. *Endocrine reviews* **21**: 697-738.
92. Hajer, G. R., T. W. van Haeften, and F. L. Visseren. 2008. Adipose tissue dysfunction in obesity, diabetes, and vascular diseases. *European heart journal* **29**: 2959-2971.

Appendix

Table 3. TAG fatty acid composition in epididymal WAT and perirenal WAT

	Wildtype Epididymal WAT	*Agpat4*$^{-/-}$ Epididymal WAT	*Wildtype* Perirenal WAT	*Agpat4*$^{-/-}$ Perirenal WAT
C 14:0	4.61	10.52	4.30	4.52
C 16:0	121.02	221.87	94.95	92.08
C 17:0	1.23	1.65	0.94	0.75
C 18:0	11.80	18.10	13.33	10.09
C 20:0	0.49	0.76	0.60	0.52
C 22:0	0.67	0.72	0.32	0.27
C 24:0	1.86	2.89	0.31	0.36
Total SFA	141.68	256.50*	114.75	108.59
C 16:1	6.00	13.50	9.92	13.52
C 18:1n-7	2.85	5.49	6.08	5.45
C 18:1n-9	36.13	63.11	82.49	73.33
C 20:1n-9	5.25	11.36	4.07	2.10
C 22:1n-9	0.69	1.02	0.35	0.34
C 24:1n-9	1.04	2.20	0.31	0.28
Total MUFA	51.96	96.69*	103.21	95.01
C 18:2n-6	0.77	1.41	12.32	7.49
C 18:3n-6	0.06	0.06	0.01	0.02
C 20:2n-6	0.22	0.29	0.07	0.06
C 20:3n-6	0.09	0.10	0.01	0.02
C 20:4n-6	0.08	0.10	0.02	0.02
C 22:2n-6	0.06	0.05	0.01	0.02
C 22:4n-6	1.37	0.41	0.28	0.12
C 22:5n-6	0.19	0.20	0.05	0.13
Total N-6	2.83	2.26	12.78	7.87
C18:3n-3	0.50	0.56	0.49	0.21
C20:3n-3	0.19	0.28	0.03	0.04
C20:5n-3	0.22	0.25	0.34	0.20
C22:6n-3	3.12	5.09	0.67	0.70
Total N-3	4.02	6.17	1.52	1.15
PUFAs	6.85	8.80	14.30	9.02
HUFAs	5.25	6.42	1.40	1.23
EPA+DHA	3.34	5.34	1.01	0.90
N-6/N-3	0.77	0.42	9.06	6.98
%n-3 HUFA	68.01	87.33	77.50	76.46
Total	200.49	361.99*	232.26	212.61